CMLS, Cell. Mol. Life Sci. 59 (2002) 193–212
1420-682X/02/020193-20 $ 1.50 + 0.20/0
© Birkhäuser Verlag, Basel, 2002

CMLS Cellular and Molecular Life Sciences

Review

Sterol carrier protein-2: structure reveals function

N. J. Stolowich [a], A. D. Petrescu [b], H. Huang [b], G. G. Martin [b], A. I. Scott [c] and F. Schroeder [b,*]

[a] Department of Chemistry, University of Louisville, Louisville, Kentucky 40292 (USA)
[b] Department of Physiology and Pharmacology, Texas A & M University, College Station, Texas 77843-4466 (USA), Fax: +1 979 862 4929, e-mail: fschroeder@cvm.tamu.edu
[c] Department of Chemistry, Texas A & M University, College Station, Texas 77843-3255 (USA)

Received 19 April 2001; received after revision 2 July 2001; accepted 31 July 2001

Abstract. The multiple actions of sterol carrier protein-2 (SCP-2) in intracellular lipid circulation and metabolism originate from its gene and protein structure. The SCP-x/pro-SCP-2 gene is a fusion gene with separate initiation sites coding for 15-kDa pro-SCP-2 (no enzyme activity) and 58-kDa SCP-x (a 3-ketoacyl CoA thiolase). Both proteins share identical cDNA and amino acid sequences for 13-kDa SCP-2 at their C-termini. Cellular 13-kDa SCP-2 derives from complete, posttranslational cleavage of the 15-kDa pro-SCP-2 and from partial posttranslational cleavage of 58-kDa SCP-x. Putative physiological functions of SCP-2 have been proposed on the basis of enhancement of intermembrane lipid transfer (e.g., cholesterol, phospholipid) and activation of enzymes involved in fatty acyl CoA transacylation (cholesterol esters, phosphatidic acid) in vitro, in transfected cells, and in genetically manipulated animals. At least four important SCP-2 structural domains have been identified and related to specific functions. First, the 46-kDa N-terminal presequence present in 58-kDa SCP-x is a 3-ketoacyl-CoA thiolase specific for branched-chain acyl CoAs. Second, the N-terminal 20 amino acid presequence in 15-kDa pro-SCP-2 dramatically modulates the secondary and tertiary structure of SCP-2 as well as potentiating its intracellular targeting coded by the C-terminal peroxisomal targeting sequence. Third, the N-terminal 32 amino acids form an amphipathic α-helical region, one face of which represents a membrane-binding domain. Positively charged amino acid residues in one face of the amphipathic helices allow SCP-2 to bind to membrane surfaces containing anionic phospholipids. Fourth, the hydrophobic faces of the N-terminal amphipathic α helices along with β strands 4, 5, and helix D form a ligand-binding cavity able to accommodate multiple types of lipids (e.g., fatty acids, fatty acyl CoAs, cholesterol, phospholipids, isoprenoids). Two-dimensional ^{1}H-^{15}N heteronuclear single quantum coherence spectra of both apo-SCP-2 and of the 1:1 oleate-SCP-2 complex, obtained at pH 6.7, demonstrated the homogenous formation of holo-SCP-2.

While comparison of the apo- and holoprotein amide fingerprints revealed about 60% of the resonances remaining essentially unchanged, 12 assigned amide residues underwent significant chemical-shift changes upon oleic acid binding. These residues were localized in three regions: the juncture of helices A and B, the mid-section of the β sheet, and the interface formed by the region of β strands 4, 5, and helix D. Circular dichroism also showed that these chemical-shift changes, upon oleic acid binding, did not alter the secondary structure of SCP-2. The nuclear magnetic resonance chemical shift difference data, along with mapping of the nearby hydrophobic residues, showed the oleic acid-binding site to be comprised of a pocket created by the face of the β sheet, helices A and B on one end, and residues associated with β strands 4, 5, and helix D at the other end of the binding cavity. Furthermore, the hydrophobic nature of the previously ill-defined C-terminus suggested that these 20 amino acids may form a 'hydrophobic cap' which closes around the oleic acid upon binding. Thus, understanding the structural domains of the SCP-x/pro-SCP-2 gene and its respective posttranslationally processed proteins has provided new insights into their functions in intracellular targeting and metabolism of lipids.

* Corresponding author.

Key words. Sterol carrier protein-2; fatty acid; binding site; NMR.

Background

Sterol carrier protein-2 (SCP-2), also called nonspecific lipid transfer protein, is the most prominent member of a family of ubiquitous, lipid-binding proteins broadly distributed in eukaryotes, including mammals [review in refs 1–4], birds [5], yeast [6], and plants [7–10]. SCP-2 has postulated functions in both cholesterol and fatty acid metabolism. SCP-2 binds cholesterol [11] and in vitro assays, transfected cells, and animal studies suggest that SCP-2 functions in cholesterol uptake [2, 12, 16–20], intracellular transport [21], esterification [22, 23], and oxidation [24–26]. In addition, SCP-2 has been suggested as necessary for cholesterol formation and incorporation into lung surfactant [27], for secretion of newly synthesized cholesterol into bile [28], and for secretion of primarily lipoprotein derived cholesterol into bile [29, 30].

SCP-2 has also been found more recently to bind fatty acids and fatty acyl CoAs, and it participates in their metabolism. Human SCP-2 and plant SCP-2 homologues [7] have high affinity (K_d = 0.2–0.4 μM) [15, 31] for normal [14, 32–34] and branched chain [34] fatty acids. Both human SCP-2 and plant SCP-2 homologues [7] also bind fatty acyl CoAs, the metabolically activated forms of fatty acids, with as much as 100-fold higher affinity (K_d = 3–4 nM) than for fatty acids [15, 31]. SCP-2 functions in the uptake, oxidation, and esterification of fatty acids. It stimulates microsomal fatty acyl CoA transacylation to cholesterol esters [review in refs 2, 4, 23] and phosphatidic acid in vitro [35]. Overexpression of SCP-2 in mice infected with adenovirus containing the cDNA encoding rat SCP-2 resulted in 70% increased liver levels of total cholesterol and 60% decreased liver cholesterol synthesis [36]. Studies with transfected cells [17, 22, 35] and gene-ablated mice [15] indicate that SCP-2 and potentially other SCP-x/pro-SCP-2 gene products are involved in triacylglyceride formation. SCP-x and potentially other SCP-x/pro-SCP-2 gene products also participate in peroxisomal fatty acid oxidation [15, 37, 38]. The SCP-2 homologue in yeast [6] is induced by fatty acids.

SCP-2 levels are altered in a number of diseases where lipid metabolism is abnormal, including diabetes, Zellweger, Niemann Pick C (NPC), and atherosclerosis. Streptozotocin-induced diabetes in rats decreased liver levels of 13-kDa SCP-2 by 60–90% [39], and ovarian levels by 60% [40]. Reduced 13-kDa SCP-2 expression in the pregnant, diabetic rat was associated with pregnancy loss [41]. Zellweger patients are deficient in peroxisomes, exhibit no detectable 15-kDa pro-SCP-2 or 13-kDa SCP-2, and are deficient in very long chain fatty acid oxidation [rev. in refs 42, 43]. NPC1 disease, in which cholesterol accumulates in liver lysosomes and Golgi, is characterized by a mutation in the NPC protein, markedly reduced levels of hepatic 13-kDa SCP-2, and accumulation of lipids in lysosomes and Golgi [44]. Macrophages form cholesterol ester-rich foam cells upon treatment with acetylated low-density lipoproteins, 25-hydroxycholesterol, or acyl-CoA:cholesterol acyltransferase inhibitors [18]. Foam cells exhibit increased mRNA encoding 13-kDa SCP-2 and increased 13-kDa SCP-2 protein [18]. SCP-2 is involved in the transport of cholesterol from the endoplasmic reticulum to bile [30]. Both SCP-2 [28, 29, 45, 46] and SCP-x participate in different aspects of bile acid synthesis [47–49]. In summary, altered cellular levels of SCP-2 are associated with a variety of abnormalities in the trafficking and intracellular utilization of cholesterol and other lipids.

Although the primary structure of the SCP-x/pro-SCP-2 gene products and their posttranslational modified protein is now beginning to be understood [2, 11, 14, 31–34, 50, 51] much less is known regarding the specific secondary/tertiary protein structural domains that determine posttranslational processing, intracellular targeting, membrane interaction, and ligand binding/specificity of SCP-2 [reviews in refs 2, 52].

SCP-x/pro-SCP-2 gene structure and mRNA transcripts

A single structural SCP-x/SCP-2 gene, comprised of 16 exons and 15 introns, has been reported in humans [53, 54], mice [15], rats [55], and chickens [5] (fig. 1). The SCP-x/pro-SCP-2 gene contains two promoter regions that initiate transcription of four types of mRNA. The N-terminal promoter region of the SCP-x/pro-SCP-2 gene gives rise to two mRNA transcripts, both of which encode the 58-kDa SCP-x translation product: 2.8 kb mRNA and alternatively polyadenylated 2.2 kb mRNA. A second promoter region in the interior of the SCP-x/SCP-2 gene gives rise to an additional two mRNAs, both of which encode the 15-kDa pro-SCP-2 translation product: 1.5 kb mRNA and alternatively polyadenylated 0.9 kb mRNA.

SCP-x/pro-SCP-2 mRNA translation products are posttranslationally modified

Both SCP-x and pro-SCP-2 contain the complete 13-kDa SCP-2 in their C termini [24, 55–61]. Posttranslational

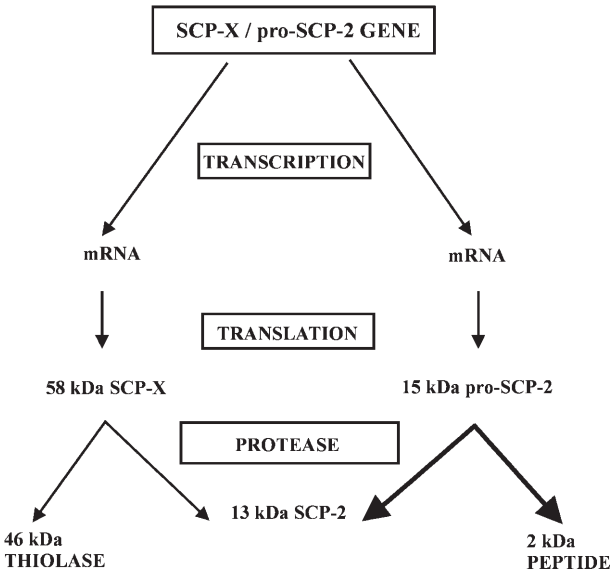

Figure 1. The SCP-x/pro-SCP-2 gene encodes two 13-kDa SCP-2 precursors.

proteolysis of either protein gives rise to the 13-kDa SCP-2. First, the 58-kDa SCP-x is partially cleaved by post-translational proteolysis of the N-terminal 1–404 amino acids (3-oxoacyl-CoA thiolase) from the C-terminal amino acid residues 425–547 which appear to be identical to 13-kDa SCP-2 [17, 62, 63] (fig. 1). However, the majority of 58-kDa SCP-x remains intact in most tissues. Second, the 15-kDa pro-SCP-2 protein translation product undergoes complete posttranslational processing (removal of the N-terminal 20 amino acids) to yield the mature 13-kDa SCP-2 (C-terminal 123 amino acids) in most tissues and cells [reviews in refs 2, 16] (Fig. 1). Incomplete cleavage has been observed, but only rarely [24, 64]. The interrelationships of the primary amino acid sequences of these proteins are summarized in figure 2. Because of this complexity, caution must be exercised in the types of antisera used for detecting these proteins in cells and tissues [review in ref. 2]. Western blotting with anti-13-kDa SCP-2 reveals only the 58-kDa SCP-x and 13-kDa SCP-2 in all tissues and almost all cell lines tested. In contrast, Western blotting with antisera raised against the 58-kDa SCP-x detects the 58-kDa SCP-x, the 46-kDa thiolase protein, and the 13-kDa SCP-2. Finally, Western blotting with antisera raised against peptides derived from the N-terminal 404-amino acid polypeptide region of the 58-kDa SCP-x detect only 58-kDa SCP-x and the 46-kDa thiolase protein.

Tertiary and secondary structure of unliganded SCP-x/pro-SCP-2 gene translation products

The physiological function(s) of SCP-x/pro-SCP-2 gene translation products are based on knowledge of the tertiary and secondary structure of the protein. This has proven to be especially important with regard to the role of the 20-amino acid N-terminal presequence in 15-kDa pro-SCP-2 [51]. While almost nothing is known regarding the tertiary or secondary structure of the 58-kDa SCP-x and the 46-kDa thiolase, high-resolution nuclear magnetic resonance (NMR) structures are available for pro-SCP-2 and SCP-2, while an X-ray structure (1.8 Å resolution) has been reported for 13-kDa SCP-2.

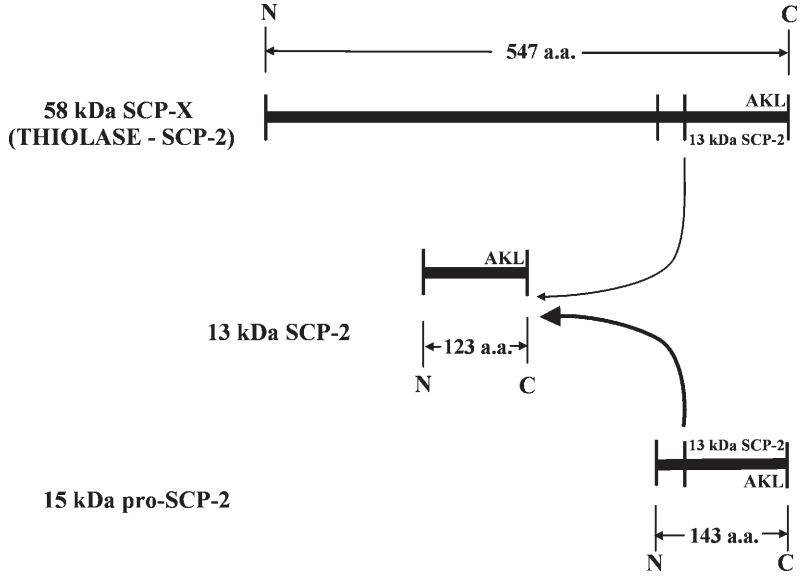

Figure 2. Primary amino acid sequence interrelationships between the 58-kDa SCP-x, 15-kDa pro-SCP-2, and SCP-2.

NMR spectroscopy

An elegant series of recent NMR studies have significantly contributed to our understanding of the tertiary and secondary structure of human apo-SCP-2 in aqueous solution [65, 66]. With the exception of the N-terminal residues 1–7 and C-terminal residues 117–123, which are flexibly disordered, the remainder of the protein is comprised of a fold formed by a five-stranded β sheet and four α helices. Computer modeling of the NMR-based structure of human apo-SCP-2 indicated a globular, slightly ellipsoidal protein with an axial ratio of 1.2–1.4 [65, 66].

The two-dimensional (2D) ^{1}H-[^{15}N]-heteronuclear single quantum coherence (HSQC) spectrum of apo-^{15}N-SCP-2 at pH 6.7 is shown in figure 3A. Excluding side chain amides and amines, 93 of 118 possible backbone amides were observed. By comparison to the previously assigned HSQC spectra of human apo-SCP-2 at pH 6 [65], very good agreement and overlap existed with the present HSQC data of apo-SCP-2 obtained at pH 6.7, indicating that little or no structural change can be detected in the pH range of 6–6.7. This resulted in the unambiguous assignment of 86 of the 93 NH cross-peaks. The remaining 7 cross-peaks could be assigned only to pairs of overlapping NH resonances. Finally, 18 NH cross-peaks, originating primarily from the C- and N-terminal ends were not observed at all under these conditions. In rabbit [66], but not human [65], apo-SCP-2, the putative lipid-binding site is covered by the C-terminal polypeptide segment 105–123. In the presence of ligand, the human holo-SCP-2 lipid binding site is uncovered [65].

Because the 15-kDa pro-SCP-2 is completely cleaved to the 13-kDa SCP-2 by posttranslational proteolysis in all tissues and almost all cells studied, relatively little attention has been paid to resolving the structure of this protein. The NMR structure of rabbit apo-15-kDa pro-SCP-2 was recently compared to that of human apo-13-kDa SCP-2 [67]. Based on nuclear Overhauser effects (NOEs), the conclusion was drawn that all secondary structures present in human SCP-2 are also present in rabbit SCP-2 and that there was no difference in the structure between these proteins. In contrast, when the structure of human apo-15-kDa pro-SCP-2 was compared di-

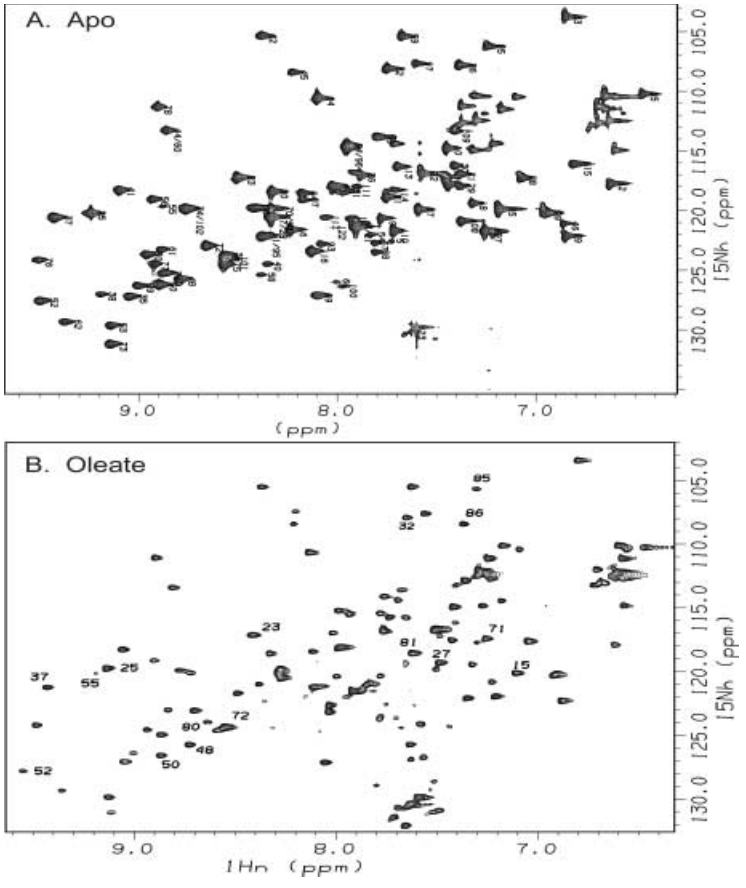

Figure 3. 500-MHz ^{1}H-[^{15}N]-HSQC spectra ^{15}N-labeled SCP-2. (*A*) Spectrum obtained from apo-SCP-2, with the amino acid residue assignments indicated based on those described earlier [65]. (*B*) Spectrum of the holoprotein obtained from the 1:1 complex of [1-^{13}C]-oleate:SCP-2 at pH 6.7. The numbered cross-peaks represent only those assigned residues which have shifted significantly (see text for complete details).

rectly with that of human apo-13-kDa SCP-2, the structures of these proteins revealed by other techniques differed significantly. The presequence dramatically altered the secondary structure of SCP-2, as ascertained by circular dichroism such that the human apo-15-kDa pro-SCP-2 exhibited threefold less α helix and sevenfold more β structure than the human apo-13-kDa SCP-2 [51]. The presequence also significantly altered the tertiary structure of SCP-2 as ascertained by carboxypeptidase A/mass spectroscopy and antibody accessibility. The human apo-15-kDa pro-SCP-2 exhibited a sixfold more reactive C terminus to carboxypeptidase A than that of human apo-13-kDa SCP-2. The human apo-15-kDa pro-SCP-2 also had twofold less binding of anti-13-kDa SCP-2 antibodies and did not enhance sterol transfer from plasma membranes as compared to human apo-13-kDa SCP-2 [51]. The functional significance of the dramatically greater accessibility of the C-terminal AKL peroxisomal-targeting sequence in the apo-15-kDa pro-SCP-2 relates to the crucial role of the N-terminal domain of the protein in regulating the exposure of the C-terminal peroxisomal-targeting site of the protein [51]. This was confirmed by immunofluorescence confocal microscopy of cells transfected with the cDNAs encoding the 15-kDa pro-SCP-2 versus the 13-kDa SCP-2 [51]. These important differences were not revealed by NMR spectroscopy. The basis for the different conclusions is not known, but may be related in part to the following fact. (i) The rabbit SCP-2 differs by three residues (Gly^4, Leu^{80}, Lys^{120}) as compared to human SCP-2 (Ser^4, Phe^{80}, Asn^{120}). (ii) The SCP-2 concentration range for NMR studies is in the millimolar range while that for fluorescence and circular dichroism is several orders of magnitude lower. The physiological concentration of SCP-2 ranges from 1 to 40 µM, depending on the tissue examined [2]. (iii) The NMR studies did not resolve the structures of the N- and C-terminal amino acid residues in either rabbit pro-SCP-2 or human SCP-2. Sequential ^{15}N and ^{1}H backbone resonances were assigned to 105 out of 143 amino acid residues in the rabbit pro-SCP-2, with the N-terminal 20 amino acids as well as some of the C-terminal amino acids being flexibly disordered [67]. Likewise, sequential ^{15}N and ^{1}H backbone resonances were assigned to amino acids 8–116 in the 123-amino acid human SCP-2 polypeptide, with the N-terminal residues 1–7 as well as C-terminal residues 117–123 being flexibly disordered [65, 66]. These results clearly indicate the importance of comparing the structure of apo-15-kDa pro-SCP-2 with that of apo-13-kDa SCP-2 by means of multiple techniques, each of which may offer additional insights.

X-ray crystallography

The rabbit recombinant apo-SCP-2 has been crystallized [68] and its X-ray crystal structure reported at 1.8-Å resolution [69]. The X-ray structure confirms the unique α/β fold obtained by NMR spectroscopy (see above). The crystal structure of the rabbit apo-SCP-2 shows that the core of the protein forms a five-stranded β sheet flanked by five α helices [69]. The N-terminal helical region is characterized by a long α helix, right-angle turn, α helix motif that leads into a structurally well-defined extended β sheet. This β sheet is comprised by the first three β strands in the primary sequence, in an antiparallel configuration, followed by a short polypeptide sequence that transverses across the back of these three strands thus allowing the fourth β strand to run parallel to the first. Computer modeling suggested that a hydrophobic tunnel-like cavity, formed by the C-terminal polypeptide comprising residues 114–124, part of the β sheet, and four of the α helices, may form a putative ligand-binding site in the rabbit apo-SCP-2 [69].

While both X-ray and NMR studies agree that the overall structure of apo-SCP2 may be depicted as a globular protein in which a five stranded β sheet comprises one face and helices the other, they differ in several important points. The X-ray structure of crystalline rabbit apo-SCP-2 defines *two* α helices within the 25-residue loop between strands IV and V. In contrast, the NMR solution structure of human apo-SCP-2 defines only *one* α helix within the 25-residue loop between strands IV and V, a region previously poorly defined in the initial NMR structure. After the short, β strand V, the C terminus ends with one final α helix that transverses across the β sheet back toward helix A. However, there are substantial differences in both the position and size of the final helix in the X-ray and NMR structures. In the X-ray structure of rabbit apo-SCP-2, the final α helix (F) starts almost immediately after β strand V (104–113), while in the NMR structure of human apo-SCP-2, the last helix (D) was found to be essentially one turn (112–115).

Circular dichroism

Circular dichroism results showed that 28–32% of SCP-2 is α helix [31, 70, 71], consistent with the above NMR data showing that 35 amino acid residues (28% of apo-SCP-2) comprise the four α helices [72]. The remainder of the SCP-2 secondary structure was comprised of about 21% β sheet, 25% β turn, and 21% random coil [31].

Fluorescence

By taking advantage of the fact that 13-kDa SCP-2 contains only a single Trp residue (amino acid position 50) and no tyrosines, the intrinsic fluorescence properties of Trp^{50} could be utilized to ascertain the location of the Trp^{50} and the overall shape, and hydrodynamic radius of 13 kDa SCP-2 [31;50]. Steady state fluorescence emission spectra as well as Stern-Volmer quenching (acry-

lamide and iodide) studies revealed that the Trp^{50} was located in a hydrophobic locus. According to time-resolved fluorescence spectroscopy of Trp^{50}, 13-kDa SCP-2 (isolated from bovine liver) exhibited a rotational correlation time of 15 ns [50]. In contrast, phase- and modulation-resolved fluorescence spectroscopy of Trp^{50} in human recombinant 13-kDa SCP-2 showed a significantly smaller rotational correlation time near 7.8 ns, consistent with SCP-2 being a globular protein with a hydrodynamic radius of 20.5 Å, diameter 41 Å [31]. This rotational correlation time was in agreement with that obtained by NMR, 7.0 ns [66]. Likewise, this diameter of SCP-2 was consistent with that determined by photon correlation spectroscopy (laser light-scattering technique), 36.0±1.2 Å [14]. This latter diameter was consistent with SCP-2 being a monomeric, slightly ellipsoidal protein. Furthermore, this diameter was in good agreement with that obtained by fluorescence phase and modulation fluorometry, 41 Å [31]. Since dimers of the human SCP-2 showed a rotational correlation time of 15.7 ns, the discrepancy between these studies was concluded as being due to SCP-2 dimer formation at the concentrations used for the studies with bovine SCP-2 [31].

Stability of apo-13-kDa SCP-2 structure

Human apo-SCP-2 is relatively stable to temperature- and solvent-induced unfolding, as shown by the following: temperature-induced transition at 70.5 °C, solvent-induced transition at 0.82 M guanidine hydrochloride, Gibbs energy of 15.5 kJ/mol for unfolding at 25 °C [73]. Although the NMR structure of human [65] and rabbit [67] apo-SCP-2 have been reported, these NMR studies utilized pH 6.0 to resolve the structure of apo-SCP-2. This pH is far from ideal for investigating SCP-2 interactions with fatty acid ligands. First, an acidic pH near 6.0 results in near complete dissociation of the naturally occurring fatty acids, oleic acid and stearic acid, from holo-SCP-2 [33]. In contrast, oleic acid binding in the holo-SCP-2 occurs exclusively at a 1:1 molar stoichiometry at pH 6.7 [33]. Second, SCP-2-mediated ligand transfer between membranes is inhibited by acidic pH [74]. Therefore, circular dichroism was used to resolve if the effects of low pH were due to pH-dependent conformational changes in apo-SCP-2 structure. Representative circular dichroic spectra of human apo-SCP-2 taken over the pH range 4.5–7.5 are shown in figure 4A, indicating little change with pH. Likewise, analysis of these and additional circular-dichroic spectra at intermediate pHs (fig. 4B) indicated that apo-SCP-2 exhibited about 26% α helix, 5% 3_{10} helix, 18% β strand, 12% β turn, 5% poly(L-proline) II type 3_1 helix, with the remainder as other structures. Reducing the medium pH from 7.5 to 4.5 had no effect on apo-SCP-2 secondary structure (fig. 4B). Additionally, comparison of ^{1}H-^{15}N HSQC data taken of

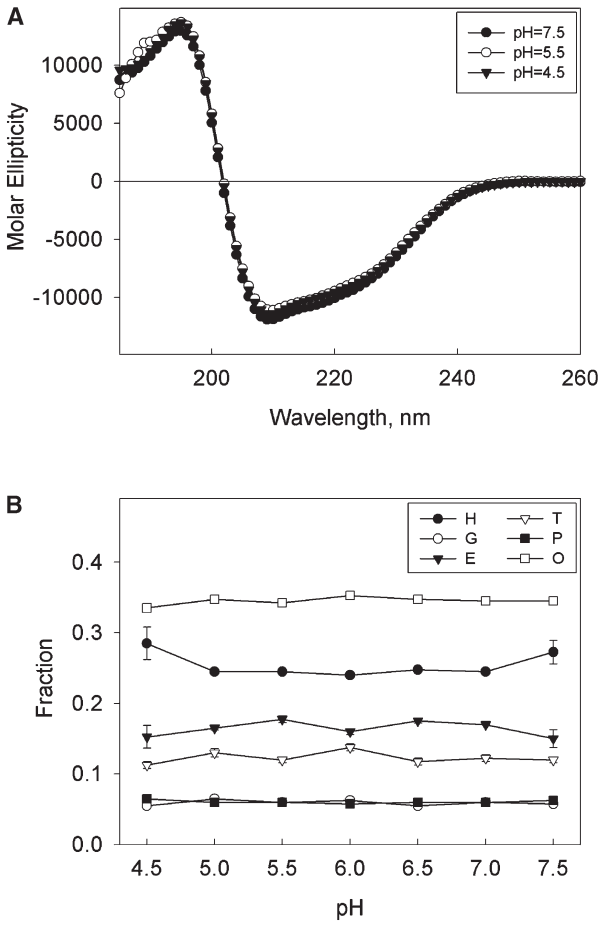

Figure 4. Effect of acidic pH on circular dichroic spectra of human apo-SCP-2. SCP-2 concentrations were 4 µM in 10 mM NaH_2PO_4/ Na_2HPO_4 or 10 mM citric acid/ Na_2HPO_4. (*A*) Closed circles, pH 7.5; open circles, pH 5.5; inverted triangles, pH 4.5. (*B*) H, α helix; G, 3_{10} helix; E, β strand; T, β turn; P, poly(L-proline)II type 3_1 helix; O, other.

apo-SCP-2 at pH 6.7 and pH 6.0 (not shown) were nearly superimposable. Taken together, these data suggested that apo-SCP-2 did not undergo significant changes in secondary structure in the pH range between 6 and 6.7, and would therefore not complicate comparison of studies performed at pHs different from that for optimal (pH 6.7) binding of naturally occurring fatty acids to SCP-2.

Tertiary and secondary structure of the liganded SCP-x/pro-SCP-2 gene translation products

Almost nothing is known regarding the ligand-binding sites of 58-kDa SCP-x or the 46-kDa thiolase. In contrast, SCP-2 has broad ligand specificity (binding fatty acids, fatty acyl CoAs, phospholipids, and sterols) and recent data show that pro-SCP-2 also binds most of these ligands.

Fatty acid-binding site: NMR

Compared to the fluorescence and circular-dichroic approaches, NMR techniques require the use of 3000-fold and 150-fold, respectively, higher SCP-2 concentrations (>0.3 mM) and correspondingly higher fatty acid concentrations to examine the SCP-2 fatty acid/fatty acyl CoA-binding site(s). ^{13}C-NMR spectroscopy of stearic acid showed that this fatty acid bound to human SCP-2 with 1:1 stoichiometry (fatty acid: protein) [14, 33]. The observation of a single fatty acid-binding site (with stearic acid) by NMR was consistent with fluorescence studies showing only a single binding site for fluorescent fatty acids [reviews in refs 31, 32, 52]. Fluorescent fatty acyl CoAs also bound at only a single binding site in SCP-2 [review in ref. 32]. In contrast, ^{13}C-NMR spectroscopy of oleic acid and oleoyl CoA showed that these ligands both bound to human SCP-2 with 2:1 stoichiometry [14, 33]. Binding of ligand at both sites increased the size distribution of SCP-2, determined by photon correlation spectroscopy, by 11% from 36.0 ± 1.2 to 40.0 ± 1.0 Å ($p<0.05$) to make the protein slightly more ellipsoidal [14]. Although the basis for the discrepancy in the number of binding sites determined by fluorescence and NMR (i.e. at least for stearic acid) versus NMR studies of oleate and oleoyl CoA binding to SCP-2 is not known, it appears associated with the high concentrations of protein and/or ligand needed for NMR studies. For example, a similar discrepancy has been observed with another fatty acid-binding protein, where additional fatty acid-binding sites were obtained with NMR studies as opposed to fluorescent fatty acid or isothermal titration calorimetry measurements of fatty acid binding to L-FABP [75].

Specificity of the [1-^{13}C]-oleic acid binding to human SCP-2 was examined using a [1-^{13}C]-oleic acid-SCP-2 complex in which both fatty acid sites were saturated [14]. Displacement was detected by monitoring the ^{13}C signal for SCP-2-bound [1-^{13}C]-oleic acid versus free [1-^{13}C]-oleic acid upon addition of increasing unlabeled oleoyl CoA or cholesterol. Oleoyl CoA completely displaced both equivalents of SCP-2-bound [1-^{13}C]-oleic acid. In contrast, cholesterol displaced only one equivalent of SCP-2-bound [1-^{13}C]-oleic acid. This suggested that while the two oleic acid-binding sites in SCP-2 also bound oleoyl CoA, only one oleic acid/oleoyl CoA-binding site also bound cholesterol.

To resolve the orientation of the fatty acid in the human SCP-2 binding site (the carboxylate oriented in the interior of the SCP-2 binding pocket or with the carboxylate of the fatty acid oriented to the surface opening), ^{13}C-NMR spectroscopy and pH titrations were performed with SCP-2-bound 1-^{13}C-stearic acid and 1-^{13}C-oleic acid. Both fatty acids were bound to SCP-2 with the carboxylate near the surface of the protein [33]. This orientation was confirmed by repeating the study with fatty acid labeled at its methyl terminal, e.g., [18-^{13}C]-stearic acid, for which pH changes over the same range did not shift the ^{13}C signal of the SCP-2-bound [18-^{13}C]-stearic acid. It should be noted that, while a preliminary study from our laboratory suggested earlier that the secondary structure of SCP-2 was significantly dependent on pH below pH 7 [33], the data in figure 4 clearly showed that the secondary structure of SCP-2 was not altered over the pH range 4.5–7.5.

As indicated above, under NMR conditions, SCP-2 exhibits as much as two fatty acid-binding sites, depending on the type of fatty acid. Furthermore, the two sites differ in ligand specificity. One site accommodates only fatty acids and fatty acyl CoAs, while the other site accommodates not only fatty acids and fatty acyl CoAs but also molecules such as cholesterol that have a larger cross-sectional area than does a fatty acid. This situation creates difficulty in using NMR spectroscopy to identify the specific amino acid residues comprising each of these fatty acid-binding sites. A portion of the residues comprising the rabbit SCP-2 fatty acid-binding site(s) were identified by examining 16-doxylstearic acid-induced shifts in the ^{15}N signals of specific amino acid residues in the rabbit holo-^{15}N-SCP-2 polypeptide chain (containing bound 16-doxylstearic acid) [66]. The nitroxide spin label bleaches (line broadening) residues within a 5-Å range. Most affected by the nitroxide spin label were amino acid residues located in helices A and C, the loop linking helix C and β strand V, and the C-terminal polypeptide segment 110–123. Trp^{50} was not affected, consistent with this amino acid being distant (40 Å) from the fatty acid-binding site [34]. These observations were used to construct a model of the binding site – a tunnel-like cavity lined almost exclusively by hydrophobic amino acids. Modeling by comparison with the known structure of human apo-^{15}N-SCP-2 suggested that in the unliganded rabbit apo-SCP-2, the lipid-binding site was covered by the C-terminal segment 105–123 [66].

While the above results represent the first data showing several of the SCP-2 amino acid residues within 5 Å of the 16-doxylstearic acid nitroxide group, there are several concerns regarding the use of the 16-doxylstearic acid to probe the fatty acid-binding site structure of SCP-2. (i) Unlike naturally occurring fatty acids, 16-doxylstearic acid is dipolar, i.e., polar moieties are located near both ends of the alkyl chain. Dipolar fatty acids (e.g., hexadecanedioic acid) bind sixfold less effectively and with the polar carboxylate oriented into the binding pocket of human holo-SCP-2 [33]. In contrast, physiologically significant and naturally occurring fatty acids (oleic acid and stearic acid) orient with the carboxylate at the surface of the protein [33]. Which orientation 16-doxylstearic acid adopts in the rabbit holo-SCP-2 is unclear. (ii) The 16-doxylstearic acid was bound to rabbit SCP-2 at pH 6.0 [66], a pH at which naturally occurring fatty acids (oleic

acid and stearic acid) are almost completely dissociated from human SCP-2 [33]. (iii) Since the chain length of 16-doxylstearic acid is about 18 Å, the spin label quenches and provides only a partial (about 1/3) view of the amino acids comprising the fatty acid-binding site. It does not reveal which SCP-2 amino acid residues interact with the carboxyl half of the fatty acid chain. (iv) The 16-doxylstearic acid may not bind to SCP-2 at a single site. Although SCP-2 binds [1-^{13}C]-stearic acid at a single site, SCP-2 has two ligand-binding sites, only one of which binds naturally occurring fatty acids with high affinity at pH 6.7 [14]. Which binding site(s) 16-doxylstearic acid interacts with in rabbit holo-SCP-2 is not clear and the binding stoichiometry of SCP-2 for 16-doxylstearic acid was not reported.

To confirm that the 16-nitroxide stearate-binding site characterization actually reflected that of a naturally occurring fatty acid, oleic acid, advantage was taken of the apo-SCP-2 insensitivity to pH and its high degree of selectivity for the 1:1 oleate : SCP-2 complex near pH 6.7.

Preparation of holo-SCP-2 with bound naturally occurring ligand

Escherichia coli expressing SCP-2 was grown in M9 minimal medium (supplemented with 2 g/l glucose, 1 mM ($MgSO_4$, 0.1 mM $CaCl_2$, 10 mg/l thiamine and 100 mg/l ampicillin) at 37 °C until the optical density at 600 nm of the bacterial suspension became 0.6. Then, isopropyl thio-b-D-galactoside IPTG (0.5 mM final concentration) was added to induce protein synthesis and ^{15}N-labeled ammonium sulfate (1 g/l) was added as a source of nitrogen. The bacterial cells were then further grown at 37 °C for 3 h, then ^{15}N-labeled SCP-2 was purified as previously described for unlabeled SCP-2 [76], modified as follows: Bacterial cells were lysed with a French press in 10 mM potassium phosphate buffer, pH 6.8, containing 2 mM dithiothreitol (DTT) and 1mM EDTA as well as complete TM protease inhibitor cocktail (as recommended by the manufacturer) plus pepstatin A (0.3 mg/100 ml). Cell debris was removed by centrifugation at 14,000 g for 20 min. The supernatant was placed on a Sephadex G-25 column and eluted. The SCP-2-enriched protein fractions were further resolved on a Mono S column from which ^{15}N-SCP-2 and a few other positively charged contaminants were eluted with a gradient of 0–1 M NaCl. Fractions containing ^{15}N-SCP-2 were collected, concentrated by ultrafiltration and resolved on a Sephadex G-50 column to yield protein over 95 % pure as assayed by Coomassie Blue staining of tricine-SDS-polyacrylamide gels [77]. Stock solutions of apo-^{15}N-SCP-2 were prepared and subjected to several buffer exchanges in NMR buffer 20 mM KH_2PO_4, 4 mM perdeuterated DTT (DTT-d_{10}), 0.1 mM EDTA, 50 µM PMSF, pH 6.7 containing 10 % D_20] employing a 3 ml stirred cell (YM5 membrane; Amicon) as described earlier for apo-SCP-2 [33]. Samples of ^{15}N-SCP-2 bound with one equivalent of [l-^{13}C]-oleic acid were prepared in similar fashion to the apoprotein, except on the final buffer exchange, when 1 mM sodium [l-^{13}C]-oleate was added to the NMR buffer, and after a 30-min incubation, the solution was concentrated to 0.5 ml resulting in a final ^{15}N-SCP-2 concentration of 1.5 mM. ^{13}C-NMR height and linewidth analysis of the enriched C-1 signal originating from the bound [l-^{13}C]-oleate [33] indicated that [l-^{13}C]-oleate-^{15}N-SCP-2 complexes prepared in this fashion reproducibly contained 1 equivalent of bound [l-^{13}C] oleate with little (< 10 %) free [l-^{13}C]-oleate present. Five hundred-mega Herz ^{1}H-[^{15}N]-HSQC spectra of 2 mM human SCP-2 (20 mM KP buffer, 4 mM DTT-d_{10}, pH 6.7) were recorded at 30 °C on a Bruker ARX-500 NMR spectrometer in a 5-mm inverse probe. 2D ^{1}H-[^{15}N]-HSQC spectra were obtained using a modified Bruker TPPI sequence employing DANTE suppression of the solvent water peak. Typically, 512 (t_2) × 128 (t_1) matrices were collected. The raw data were processed using either XWlN-NMR (Bruker) or FELIX (MSI) software via zero filling and linear prediction of the ^{15}N dimension to 256 points and apodization with Gaussian function in both dimensions. Peak picking and data analysis were accomplished using FELIX.

2D ^{1}H-[^{15}N]-HSQC spectrum of l:l oleic acid: ^{15}N-SCP-2 complex

Taking advantage of the insensitivity of apo-SCP-2 to pH described above [33] allowed not only determination of the l:l oleate:^{15}N-SCP-2 structure but also permitted direct comparison with the apo-^{15}N-SCP-2 NMR structure also obtained at pH 6.7 (fig. 3 A). The 2D ^{1}H-[^{15}N]-HSQC spectrum of l:l oleate: ^{15}N-SCP-2 complex at pH 6.7 (fig. 3 B) was found to be homogenous, with linewidths comparable to those of the apoprotein, indicating that a uniform, tight-binding complex between oleate and ^{15}N-SCP-2 had been obtained. Excluding side chain NH cross-peaks, 112 of 118 cross-peaks were identified (20 more than in the case of the apoprotein) suggesting a more ordered structure relative to the apo-SCP-2.

Comparison of the chemical shift differences between apo and holo ^{15}N-SCP-2

Careful comparison of the amide nitrogen 'fingerprints' (table 1, fig. 5 A) of the apo-^{15}N-SCP-2 and holo-^{15}N-SCP-2 forms as well as comparison of the amide proton 'fingerprints' (fig. 5 B) of the apo-^{15}N-SCP-2 and holo-^{15}N-SCP-2 forms allowed determination of the effect of oleate binding on the overall structure of SCP-2. Approximately 1/3 of the observed cross-peaks fell into the type I assignment category, i. e., amino acid residues in which little or no significant chemical shift differences were observed between apo-^{15}N-SCP-2 and holo-^{15}N-SCP-2 containing bound oleate. These peaks varied less than one

Table 1. Effect of oleic acid binding on backbone amide chemical shifts of human SCP-2.

Residue	ΔH	ΔN	Type[1]	Effect[2]	Secondary[3]
Lys8	nd	nd	III		helix A
Ala9	−0.04	0.11	II	*	helix A
Asn10	−0.02	0.18	I		helix A
Leu11	nd	nd	III		helix A
Val12	0.01	0.21	I		helix A
Phe13	nd	nd	III		helix A
Lys14	nd	nd	III		helix A
Glu15	−0.06	0.26	II	*	helix A
Ile16	nd	nd	III		helix A
Lys18	0.02	0.08	I		helix A
Lys19	nd	nd	III		helix A
Leu20	0.01	0.16	I		helix A
Glu21	0.03	0.20	I		helix A
Glu22	−0.05	−0.15	II	*	helix A
Glu23	−0.07	−0.08	II	*	helix B
Gly24	0.05	0.11	II	*	helix B
Glu25	−0.09	−0.58	II	***	helix B
Gln26	nd	nd	III		helix B
Phe27	−0.09	−0.58	II	***	helix B
Lys29	nd	nd	III		helix B
Lys30	0.01	−0.04	I		helix B
Ile31	nd	nd	III		helix B
Gly32	−0.08	−0.17	II	**	strand I
Gly33	−0.04	−0.25	II	*	strand I
Ile34	0.03	0.10	I		strand I
Phe35	0.01	−0.05	I		strand I
Ala36	nd	nd	III		strand I
Phe37	0.03	0.67	II	**	strand I
Lys38	−0.07	−0.15	II	*	strand I
Val39	0.01	0.13	I		strand I
Lys40	−0.04	−0.06	I		strand I
Asp41	−0.03	0.03	I		
Gly42	0.00	0.20	I		helix C
Gly45	0.00	0.05	I		helix C
Lys46	−0.01	0.01	I		helix C
Glu47	nd	nd	III		
Ala48	−0.05	0.02	II	*	strand II
Thr49	nd	nd	III		strand II
Trp50	−0.01	0.40	II	*	strand II
Val52	0.07	0.28	II	*	strand II
Asp53	−0.00	0.25	I		strand II
Val54	nd	nd	III		strand II
Lys55	0.31	0.52	II	*****	
Asn56	−0.01	0.15	I		
Lys58	nd	nd	III		
Gly59	−0.03	0.16	I		
Val61	−0.04	−0.18	II	*	strand III
Leu62	−0.01	−0.10	I		strand III
Asn64	nd	nd	III		
Ser65	0.01	−0.03	I		
Asp66	nd	nd	III		
Lys67	−0.05	−0.22	II	*	
Lys68	−0.02	0.13	I		
Ala69	−0.03	0.03	I		
Cys71	−0.12	0.45	II	**	strand IV
Thr72	0.01	1.01	II	**	strand IV
Ile73	−0.02	0.01	I		strand IV
Thr74	0.01	−0.26	I		strand IV
Met75	nd	nd	III		strand IV
Ala76	−0.02	0.07	I		strand IV
Asp77	0.02	0.09	I		helix D
Ser78	0.00	−0.19	I		helix D
Asp79	0.05	0.18	II	*	helix D
Phe80	−0.25	0.62	II	*****	helix D
Leu81	−0.12	−0.27	II	**	helix D

Table 1 (continued)

Residue	ΔH	ΔN	Type[1]	Effect[2]	Secondary[3]
Ala82	nd	nd	III		helix D
Leu83	nd	nd	III		helix D
Thr85	0.08	−0.48	II	**	helix D
Gly86	0.00	0.64	II	*	
Lys87	−0.07	0.07	II	*	
Met88	−0.03	0.38	I		
Ala93	−0.04	−0.12	I		helix E
Gly97	−0.03	−0.03	I		
Leu99	−0.03	0.04	I		
Lys100	nd	nd	III		strand V
Ile101	nd	nd	III		strand V
Thr102	0.04	0.30	II	*	strand V
Leu107	nd	nd	III		helix F
Ala108	0.13	0.03	II	**	helix F
Met109	0.00	−0.11	I		helix F
Lys110	nd	nd	III		helix F
Leu111	nd	nd	III		helix F
Asn113	nd	nd	III		helix F
Leu114	nd	nd	III		
Gln115	nd	nd	III		
Leu116	−0.08	−0.22	II	*	
Leu123	0.03	0.07	I		

[1] Assignment types as described in the text.
[2] * to ***** represent the number of standard deviation (SD = linewidth) shifts on binding oleate.
[3] Secondary structure as determined in X-ray analysis [39].

peak width, i.e., either partially or totally overlapping the original peak position. Next, approximately 1/3 of the cross-peaks fell into the type II assignment category, comprising amino acids that experienced moderate to significant chemical shift differences (more than one linewidth SD) between the apo- and holo-^{15}N-SCP-2 forms. Finally, the last third of cross-peaks fell into the type III assignment category characterized by either absent peaks or peaks shifted in a crowded area in which their assignment was no longer possible. The key amino acid shifts in holo-SCP-2 containing bound oleic acid are also shown in ribbon diagram form in figure 6A. To illustrate the potential hydrophobic binding surface, the side chains of the adjacent hydrophobic residues are included in figure 6B.

Computer modeling of holo-SCP-2 based on comparison of the chemical shift differences between apo and holo ^{15}N-SCP-2

As shown above, the NMR data demonstrated that human holo-SCP-2 complexed in stoichiometric fashion with a naturally occurring fatty acid, oleic acid, and exhibited localized, but not global, structural changes. In comparing the observed chemical shift differences between apo-^{15}N-SCP-2 to that of holo-^{15}N-SCP-2 containing bound oleate, and then relating these changes to primary and secondary structure, the following observations were made.

The region with the highest degree of *overall* conserved structure encompassed the sequence between residues 34–77. This region, comprised of β strands I–IV and α helix C, scored the highest number of cross-peaks that did not significantly shift on binding oleate (type I), while having also the fewest number of type II and type III cross-peaks. Only amino acids Phe^{37}, Lys^{55}, Cys^{71}, and Thr^{72} showed medium or large chemical differences on binding oleate. These significantly shifted residues are highlighted in black in the space-filling cartoon diagram of SCP-2 (fig. 7A) which represents a qualitative model based on NMR structural data presented here and earlier [65].

Two regions accounted for the highest number of cross-peaks experiencing mid and large chemical shift changes associated with binding. The first of these two regions began at the end of helix A and ran through the beginning of β strand I, with the largest variance in α helix B, particularly Glu^{25} and Phe^{27}. Helix A also displayed a high number of type III cross-peaks, peaks which could not be assigned after binding oleate. The second region that experienced a high frequency of mid and large chemical shift differences was essentially the entire sequence between residues 79–90. This region, whose tertiary structure in the human apo-SCP-2 was previously not defined by NMR [65], is composed primarily of α helix D as defined in the X-ray structure.

Essentially the entire remaining holo-SCP-2 C-terminus beyond Lys^{100} underwent significant changes and contains the highest number (18) of residues that could not be assigned. Once again, this region was not defined in the

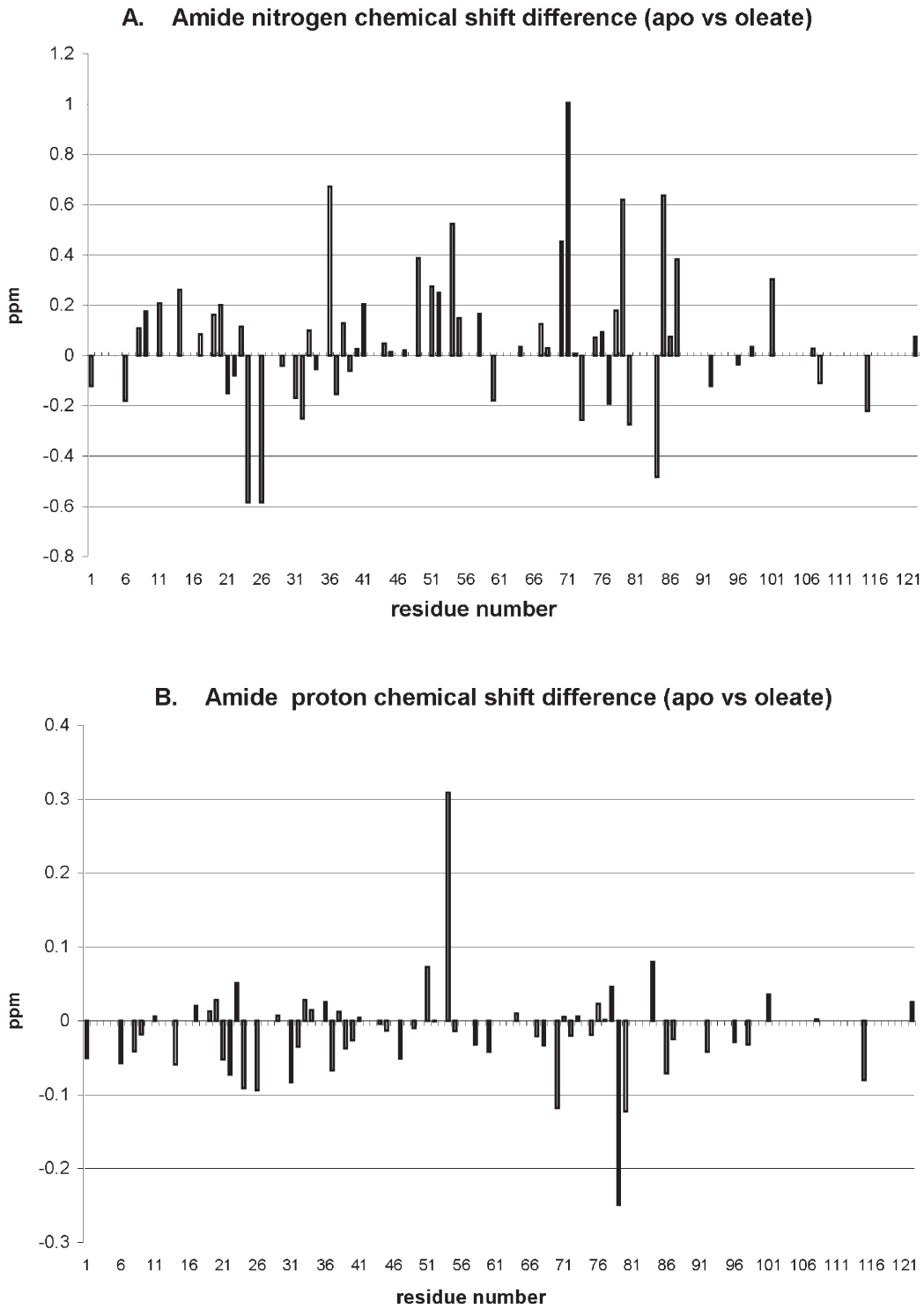

Figure 5. Chemical shifts in 500-MHz ^{1}H-[^{15}N]-HSQC spectra of ^{15}N-labeled SCP-2 upon oleic acid binding. Plot of chemical shift difference between apo-SPC-2 and oleate-SPC2 complex versus residue number for the amide nitrogens (*A*) and the amide protons (*B*) derived from the 2D HSQC spectra shown in figure 4.

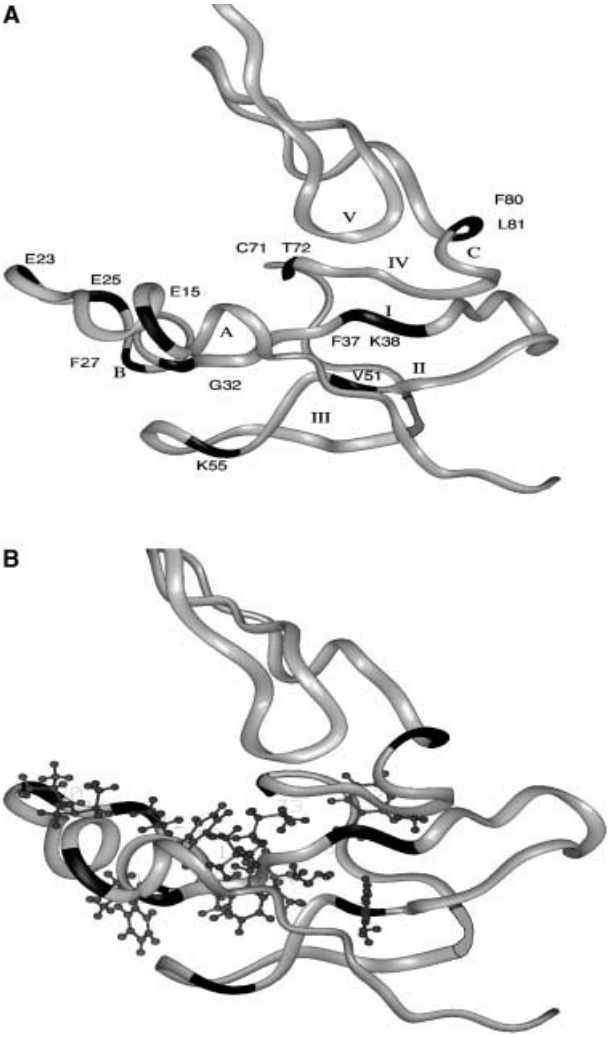

Figure 6. Backbone ribbon representation of apo-SCP-2, with the residues that undergo significant chemical shift changes on binding oleate highlighted in black. (*B*) As in (*A*), however with the side chains of the adjacent hydrophobic residues included to illustrate the potential hydrophobic binding surface.

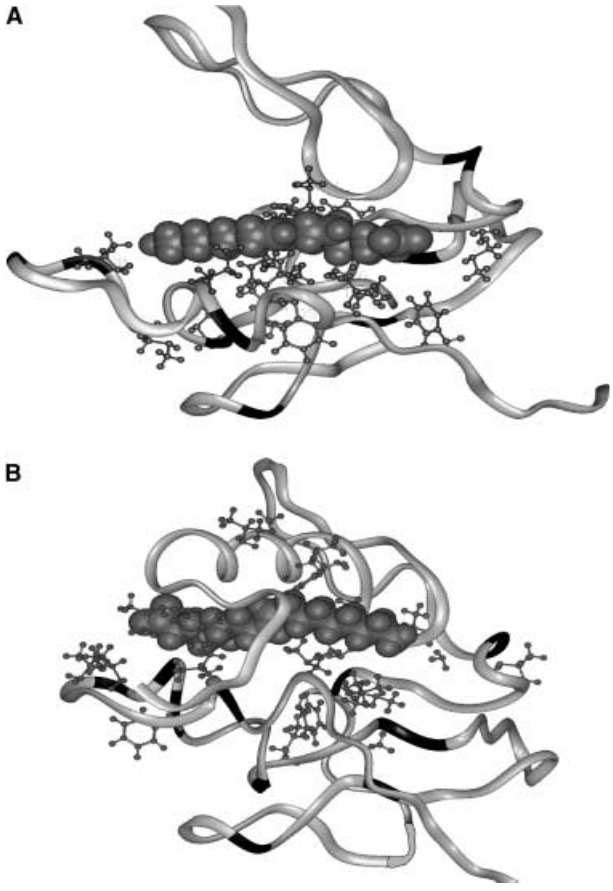

Figure 7. Space-filling model of oleic acid placed within the putative fatty acid-binding site of SCP-2. (*A*) Placement of oleic acid within the binding cavity of SCP-2 formed by the β sheet in the background and helix A in the foreground. The undefined C terminus is shown pointing towards the top of the figure, away from the binding cavity. (*B*) The C terminus has been modeled to close on the top of the binding cavity. The orientation of the fatty acid depicted has its terminal methyl end to the left hand side (helix A-turn-helix B), while the carboxylate is at the right hand side, near helix C.

initial NMR structure [65], indicating that the C terminus of the apo-SCP-2 is highly disordered in solution.

Finally, the circular dichroic spectra of SCP-2 and the relative proportions of the respective secondary structures resolved by this method were basically unaltered in the presence of oleic acid. These data would indicate that the above NMR-based alterations were due to alterations in tertiary structure and/or local alterations not detectable by circular dichroism.

These results, when taken together with the recent refined 3D structures of the apoprotein determined by NMR and X-ray analysis [65, 66, 68, 69], and secondary structure determined by circular dichroism [31, 70, 71] suggest the following model of fatty acid ligand binding.

First, the planar structure of the extended β sheet motif of apo-SCP-2 remained unperturbed by binding of oleate. This is suggested by the observation that relatively few amide resonances in this region had undergone significant chemical shift perturbations. On the other hand, most of the α-helical structures of SCP-2 appear to be sensitive to the binding of oleate, leading to the following binding site proposal. The extended fatty acid-binding site is envisioned to begin in the pocket formed by the end of helix A, helix B, and the short loop connecting strand I. This was further supported by the observation that most of the amide cross-peaks with the greatest shifts were clustered in these areas. For example, Glu^{25} and Phe^{27} in helix B underwent substantial changes, along with minor changes at residues 32 and 33 (fig. 6A). Quite interestingly, this pocket (formed by helix A and B and the beginning of β strand I and the end of strand II) was comprised of primarily hydrophobic amino acids. For example, the se-

quence between Phe[27] and Phe[37] is comprised of all nonpolar residues, with the exception of the two lysines at positions 29 and 30. These two lysines lie at the back of helix B and hence face away from the pocket, toward outside solvent. Moreover, the nearby adjacent sequence of β strand II contained three valines (amino acids 51, 52, and 54) which could participate in the hydrophobic binding pocket. The impact of the number of hydrophobic residues near the proposed binding cavity is illustrated in figure 6B, in which the side chains of key hydrophobic residues (alanine and larger) were added to the backbone ribbon structure depicted in figure 6A. Additionally, a second particularly hydrophobic region of nonpolar residues was found at the beginning of helix A, extending several hydrophobic residues into the proposed binding pocket. Furthermore, many assignments in helix A were 'lost' upon binding oleate, suggesting movement of helix A, perhaps closing upon binding oleate.

Second, the fatty acid-binding site then transverses away from helix A, across β strands II and III and presumably exits into the area of strands IV and V. This was the second region of highly clustered, significantly shifted residues that were observed on binding oleate. Notable changes in this region include Cys[71] and Thr[72], which neighbors Asp[70] (fig. 6A). Both residues 70 and 71 have been implicated as being essential for lipid transfer activity in site-specific mutagenesis studies [72]. Not surprisingly, residues 71–76 are once again comprised of nonpolar amino acids.

Third, there was an indication that the region just after strand IV which contains helices C, D, and E, may undergo a significant conformational change as suggested by minor or major chemical shift differences in every cross-peak from residue 78 (the start of helix D in the rabbit structure) to residue 88 (fig. 6A). In the previous NMR structure of the apo-SCP-2, the 3D structure of this region (and location of helix D) was not solved, indicating that the region between residues 78–100 was conformationally mobile. The fact that large backbone amide chemical shifts in helix D and ensuing residues 85–88 were observed on binding oleate, and that helix D was comprised of essentially all hydrophobic residues, suggested that this region may have reoriented or closed around the ligand. In the X-ray structure of the apoprotein, Met[84] along with nearby Phe[37] and Ile[16] form the basis of the entrance of a hydrophobic tunnel. Additionally, Met[84] was proposed to rotate to open up the tunnel. Alternatively, the NMR data suggest that helix D may be mobile enough to move sufficiently to expose the hydrophobic tunnel.

Fourth, the last 20 amino acids, which had scored the highest number of type III 'non' assignments, were found to be composed primarily of hydrophobic and uncharged residues. This led to the speculation that the C terminus may reorient itself around the fatty acid ligand, thus providing hydrophobic contacts. The C-terminal 'cap' appears much more disordered in the solution structure than in the crystal, lending further support for this model. This hypothesis is shown in figure 7B, illustrating the potential fit of this hydrophobic 'cap' around the previously exposed end of the ligand (fig. 7A). This model also leads to the prediction of orientation of the bound oleic acid in the binding pocket. As shown in figure 7B, the oleic acid methyl terminal end is buried in the hydrophobic pocket formed by residues originating from strands II and III, helices A and B, along with the C-terminal 'cap' thus leaving the oleic acid carboxylate exposed near the juncture of strands IV and V. This orientation allows for the solvent accessibility of the carboxylate previously demonstrated by pH titration [33] and for interaction with one of the nearby basic residues, Lys[87], Lys[98], Lys[100], Arg[91]. Moreover, in the case of the fatty acyl CoA analogue of the fatty acid, this would predict surface binding of the CoA moiety outside the hydrophobic cavity, perhaps between helices E and F and toward the outside surfaces of β strands IV and V. Such a surface binding of the CoA moiety of fatty acyl CoAs has previously been shown for the intestinal fatty acid-binding protein, which also binds both fatty acids and fatty acyl CoAs [78–80].

Fatty acid-binding site: fluorescence

Because SCP-2 was initially reported not to bind fatty acids specifically [81], for the last decade, SCP-2 was assumed not to participate in fatty acid trafficking/metabolism. However, in 1995, binding of fluorescent fatty acids to SCP-2 was found to be very sensitive to the presence of the solvents used in the earlier assay [32, 82]. In the absence of solvent interference, SCP-2 binds naturally occurring fluorescent fatty acids with high affinity, the K_d being as low as 180 nM [15, 31–34, 51, 82, 83]. In fact, 13-kDa SCP-2 isolated from recombinant bacteria contains a small amount of endogenously bound fatty acid [33]. These discoveries not only stimulated tremendous interest in identifying potential novel physiological functions of SCP-x/pro-SCP-2 gene products in fatty acid trafficking/metabolism, but for the first time provided a tool for examining the structure of SCP-2 containing bound ligand (see below). Fluorescence spectroscopy and circular dichroism require very low concentrations of SCP-2 protein (near 0.1 µM for fluorescence, near 2 µM for circular dichroism) to analyze the fatty acid-binding site. Since cellular unesterified fatty acid levels are near 20 µM [84] and cellular SCP-2 concentrations are between 1–40 µM [85], these techniques are ideal for examining fatty acid-SCP-2 interactions and properties of the fatty acid-binding site (microenvironment) under physiological conditions and where potential ligand aggregation and/or protein dimerization are largely avoided.

The spectral properties several fluorescent fatty acids proved useful in demonstrating that (i) fatty acid was specifically bound to SCP-2 rather than just co-aggregated with the protein, and (ii) SCP-2 Trp^{50} was in close proximity to bound fatty acid. Because the fluorescence emission of tryptophan overlaps with the absorbance of cis-parinaric acid, fluorescence resonance energy transfer (FRET) was used to demonstrate that human SCP-2 Trp^{50} was located 40 Å from the fatty acid fluorophore [34].

The SCP-2 bound NBD-stearic acid was located in a very hydrophobic binding pocket with a dielectric constant near 2. This was much more hydrophobic than that sensed by NBD-stearic acid bound to other cytosolic proteins that bind fatty acids, e.g., L-FABP with a fatty acid-binding site dielectric constant near 24 [32]. The orientation of SCP-2-bound fluorescent cis-parinaric acid was examined by comparing displacement with dicarboxylic (hexadecanedioc acid) versus monocarboxylic (hexadecanoic acid) acids [33]. The displacement efficiency of the dicarboxylic fatty acid was about sixfold less than that of the monocarboxylic fatty acid, consistent with the NMR data indicating that the fatty acid preferentially binds to human SCP-2 with the carboxylate oriented to the surface opening of the SCP-2 binding pocket. However, weaker binding of fatty acid in the opposite orientation appeared possible.

The limiting anisotropy (measures order) of the naturally occurring fluorescent cis- and trans-parinaric acids bound to human SCP-2 was 0.335 ± 0.001 (equivalent to a wobbling cone angle of 18°) and 0.365 ± 0.001 (equivalent to a wobbling cone angle of 12°), respectively [31]. Thus, the straight-chain fluorescent fatty acid (trans-parinaric acid, a saturated fatty acid analogue) was significantly more ordered than the kinked-chain fluorescent fatty acid (cis-parinaric acid, an unsaturated fatty acid analogue) within the SCP-2 fatty acid-binding site.

The rotational correlation time of fluorescent fatty acids measures the mobility of the fatty acid within the binding site. Cis-parinaric acid and trans-parinaric acid bound to human SCP-2 had a rotational correlation time of 7.51 ± 0.12 ns and 8.43 ± 0.22 ns, respectively [31]. Likewise, pyrenyl-dodecanoic acid bound to bovine SCP-2 exhibited a rotational correlation time of 7 ns [83]. These data show that the bound fluorescent fatty acids rotated with a correlation time indistinguishable from that of the entire SCP-2 protein rotation, 7.8 ± 0.6 ns [31]. Taken together with the anisotropy data, these results show that SCP-2-bound fatty acid, so highly ordered and motionally restricted, rotates with the same rate as the entire hydrated protein.

Both circular dichroism and fluorescence were used to examine if fatty acid binding altered the secondary and/or tertiary structure of human SCP-2. Circular dichroic spectra of SCP-2 were not significantly altered by oleic acid, indicating that fatty acid binding did not alter SCP-2 overall secondary structure fractions [31]. The effect of oleic acid on the circular dichroic spectra of SCP-2 was determined as described above. The circular dichroic spectra of holo-SCP-2 complexed with oleic acid were not grossly altered compared to that of apo-SCP-2 (fig. 8A). Analysis of these spectra further revealed that oleic acid did not significantly alter the proportion of any of the apo-SCP-2 secondary structural components including the α helix, 3_{10} helix, β strand, β turn, poly(L-proline)II type 3_1 helix, or other structures (fig. 8B). Thus, oleic acid binding in human holo-SCP-2 did not alter the relative proportions of secondary structures present in human apo-SCP-2.

Fatty acyl CoA-binding site: NMR and fluorescence

Fluorescence binding studies showed that SCP-2 binds fatty acyl CoAs [15, 31, 83] with an order of magnitude higher affinity than fatty acids [15, 31, 83]. The human 13-kDa SCP-2 exhibits one fatty acyl CoA-binding site as determined by fluorescence binding assays with cis-parinaroyl CoA or trans-parinaroyl CoA [31]. In contrast, at the much higher protein and ligand concentrations used for NMR spectroscopy, two oleoyl CoA-binding sites were reported [14]. The mobility of fatty acyl CoA bound to 13-kDa SCP-2 was even more restricted than that of the corresponding fatty acids bound to 13-kDa SCP-2. Wobbling cone angles of bound cis-parinaroyl CoA and trans-parinaroyl CoA, 12° and 13° respectively, were 60% smaller than those of the corresponding bound fatty acids [31]. The limiting anisotropies of bound cis-parinaroyl CoA and trans-parinaroyl CoA, 0.365 and 0.361 respectively, were significantly greater (more ordered) than the corresponding fatty acids in the SCP-2 binding site [31]. Fatty acyl CoA binding significantly altered the tertiary, but not secondary, structure of SCP-2. Oleoyl CoA binding increased the rotational correlation time of SCP-2 (determined with Trp^{50} fluorescence) and increased the hydrodynamic radius of the protein by 2 Å, but did not significantly alter the SCP-2 secondary structure as determined by circular dichroism [31]. Consistent with fatty acyl CoA-induced altered tertiary structure of SCP-2, the rotational correlation times of SCP-2-bound cis-parinaroyl CoA and trans-parinaroyl CoA (8.43 ± 0.22 and 8.82 ± 0.08 ns, respectively) were significantly longer than that of the apo-protein, 7.8 ± 0.6 ns [31]. As determined by photon correlation spectroscopy, binding of oleoyl CoA to human SCP-2 significantly increased the hydrodynamic diameter by 4 Å, from 36.0 ± 1.2 to 40.0 ± 1.0 Å ($p < 0.05$) to make the protein slightly more ellipsoidal [14].

The 15-kDa pro-SCP-2 exhibited 2- to 5-fold lower affinity, but a similar pattern, for fatty acyl CoA binding as compared to 13-kDa SCP-2 [83].

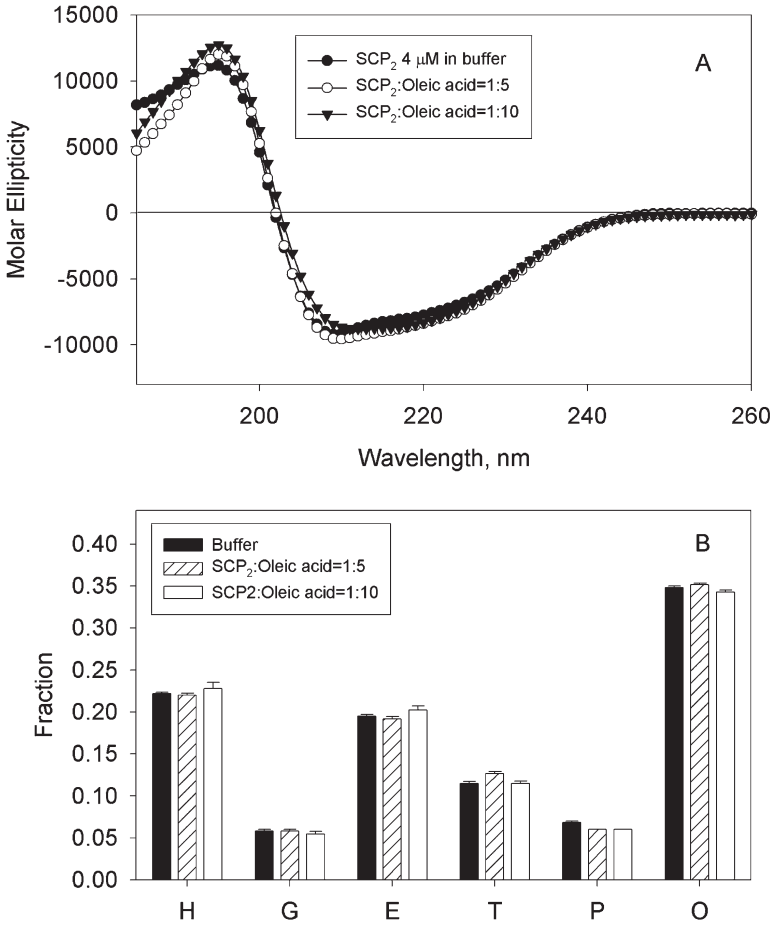

Figure 8. Effect of oleic acid binding on circular dichroic spectra of human apo-SCP-2. Circular dichroic spectra of recombinant human apo-SCP-2 and holo-SCP-2 (2 μM) dissolved in 10 mM phosphate buffer, pH 7.4, were recorded as described [51]. The circular dichroic spectra were analyzed using the program CDsstr [98, 99], using a singular-value decomposition algorithm described earlier [100]. (*A*) Closed circles, 4 μM apo-SCP-2; open circles, 4 μM apo-SCP-2 + 20 μM oleic acid; triangles, 4 μM apo-SCP-2 + 40 μM oleic acid. (*B*) Solid bar, 4 μM apo-SCP-2; cross-hatched bar, 4 μM apo-SCP-2 + 20 μM oleic acid; open bar, 4 μM apo-SCP-2 + 40 μM oleic acid. H, α helix; G, 3_{10} helix; E, β strand; T, β turn; P, poly(L-proline)II type 3_1 helix; O, other.

Cholesterol-binding site: fluorescence and NMR

The majority of reports showed that SCP-2 has a single binding site for cholesterol [12, 14, 15] and a variety of fluorescent sterols [2, 11, 12, 14, 51, 82, 86]. Depending on the type of assay used (direct vs competition), reported K_ds ranged from as low as 4.2 nM (direct binding assays) to 2.6 μM (competition assays). Relatively little is known regarding the nature and structural location of the SCP-2 sterol-binding site. FRET from native rat liver SCP-2 Trp^{50} to bound dehydroergosterol indicated that the Trp^{50} was relatively close, 13.7 Å, to the dehydroergosterol fluorophore [11], and much closer than to the cis-parinaric acid fluorophore located 40 Å from Trp^{50} [34]. These differences may be explained in part by the fact that the dehydroergosterol fluorophore is closer to the polar head group (OH) of cholesterol than the cis-parinaric acid fluorophore is to the polar head group (COO-) of the fatty acid.

Phospholipid-binding site: fluorescence

SCP-2 also binds fluorescent phospholipids [87, 88] with phosphatidylcholine (neutral charge) > phosphatidylinositol (one net negative charge) > phosphatidylinositolphosphate (two net negative charges) > phosphatidylinositoldiphosphate (three net negative charges) [88]. While most reports suggest only one phospholipid-binding site [50, 82, 89], certain phospholipids may bind at two sites [82]. SCP-2-bound fluorescent phospholipid exhibits a rotational correlation time of 7.4 ns, i.e., motionally very restricted, and it rotates with the rotation of the whole protein [50]. The relationship of the phospholipid-binding site(s) of SCP-2 to the fatty acid-, fatty acyl CoA-, and cholesterol-binding site(s) remains to be determined. Since SCP-2 binds phospholipids, it should bind both of the acyl chains present in phospholipids. By analogy, phosphatidylcholine transfer protein is totally different from SCP-2 in terms of sequence, but also binds phosphatidylcholine [90, 91]. Interestingly, fluorescence

studies demonstrated that the two fatty acyl chains of phosphatidylcholine appear to bind in orthagonally oriented hydrophobic cavities of the phosphatidylcholine transfer protein. Although SCP-2 does not share significant sequence homology with phosphatidylcholine transfer protein, it may also have two such sites. This is suggested by NMR studies showing that some ^{13}C-fatty acids bind to SCP-2 at two sites [33], but not by fluorescence techniques which show a single site (reviewed in ref. 52].

Function of the C-terminal amino acid residues in SCP-x/pro-SCP-2 translation products

The C terminus of SCP-x, pro-SCP-2, and SCP-2 contains a peroxisomal targeting sequence, AKL (fig. 2). Thus, based on amino acid sequence alone, all three proteins are expected to be peroxisomal. Indeed, the 58-kDa SCP-x is almost exclusively peroxisomal [reviews in refs 2, 17]. The 15-kDa pro-SCP-2 is not detectable in almost all tissues and cells examined. Subcellular fractionation showed that the 13-kDa SCP-2 does not co-purify with 58-kDa SCP-2 and other peroxisomal markers, while immunocytochemistry demonstrated that the 13-kDa SCP-2 is present both in (about 50%) and outside peroxisomes [reviews in refs 2, 35, 51, 52, 92].

Function of the N-terminal amino acid residues in SCP-x/pro-SCP-2 translation products

The two types of N-terminal extensions of 13-kDa SCP-2 differ markedly in function.

The N-terminal presequence in SCP-x

The N-terminal 404 amino acid presequence present in SCP-x is a 3-ketoacyl CoA thiolase enzyme [93–95]. SCP-x is partially posttranslationally cleaved to this 3-ketoacyl CoA 46-kDa thiolase (N-terminal 404 amino acids) and 13-kDa SCP-2 deriving from the C-terminal 123 amino acids [reviewed in ref. 52]. Both the 58-kDa SCP-x and 3-ketoacyl CoA 46-kDa thiolase co-purify with peroxisomes and are thought to be exclusively peroxisomal [reviewed in ref. 52]. In contrast, the 13-kDa SCP-2 is detected in peroxisomes, but does not co-purify with peroxisomes, and has been shown to be both extraperoxisomal as well as peroxisomal [reviewed in ref. 52].

The N-terminal presequence in pro-SCP-2

Although the N-terminal 20-amino acid presequence present in pro-SCP-2 does not in itself target SCP-2 to the peroxisome, it is nevertheless essential for facilitating the ability of the C-terminal AKL peroxisomal-targeting sequence to target SCP-2 to peroxisomes [51]. This presequence dramatically alters the secondary and tertiary structure of SCP-2 [51]. The pro-SCP-2 appears to be the predominant precursor of SCP-2 [reviewed in ref. 52].

Structural/functional significance of the N-terminal α-helical region of 13- kDa SCP-2

The mechanism whereby SCP-2 mediates the intermembrane transfer of various lipid species appears to require not only a ligand-binding site, but also a membrane interaction site [96]. Site-directed mutagenesis studies indicated that removal of the N-terminal 10 amino acids or replacement of Leu^{20} with Glu^{20} dramatically reduced the SCP-2 α helix content and abolished its lipid transfer activity [72]. However, whether this loss of activity was due to loss of the ligand-binding site or loss of membrane binding was not determined. Examination of the SCP-2 amino acid sequence revealed that the N terminus contained a putative amphipathic α-helical region that was postulated to represent a membrane interaction domain [97]. This possibility was subsequently confirmed through use of a group of synthetic SCP-2 N-terminal peptides along with circular dichroism and filtration assays [70, 71]. As indicated by increased α helix formation and binding (filtration binding assay), SCP-2 and the $^{1-32}$SCP-2 peptide preferentially interacted with highly curved model membranes rich in anionic phospholipids and cholesterol. While removal of the N-terminal 10 amino acids did not inhibit the ability of the $^{10-32}$SCP-2 peptide to bind to membranes and form α-helical structure, mutations in the $^{1-32}$SCP-2 peptide corresponding to truncation of the α-helical-forming region, e.g., $^{1-24}$SCP-2, or disruption of the α-helical-forming region, e.g., replacement of Leu^{20} with Glu^{20}, reduced or inhibited membrane binding and formation of α helices [70, 71]. The latter mutations in the intact SCP-2 protein also inactivated the SCP-2 in lipid transfer assays [72]. These data for the first time established that the N-terminal 32 amino acids of SCP-2 represent an amphipathic α helix that is the membrane interaction domain of the protein.

Conclusions and future perspectives

Understanding the structural features of SCP-2 is essential to resolving the multiple functions of this fascinating protein. Several structurally related features have been discovered. First, SCP-2 is not, in itself, directly encoded by the SCP-x/pro-SCP-2 gene. Instead, 13-kDa SCP-2 is a posttranslational cleavage product arising from C-terminal proteolytic cleavage of the 15-kDa pro-SCP-2 and the 58-kDa SCP-x. Second, the N-terminal presequences, while themselves not comprising either of the known peroxisomal targeting sequences (PTS-1 or PTS-2), are es-

sential for facilitating the targeting of the respective proteins via the C-terminal AKL (PTS-1 targeting sequence) to peroxisomes. Third, the N-terminal presequence of SCP-x is a 3-ketoacyl CoA thiolase specifically involved in the peroxisomal oxidation of branched-chain fatty acids. Fourth, the N-terminal 32 amino acids of 13-kDa SCP-2 represent an amphipathic α-helical domain that is essential for interaction with anionic phospholipid-containing membranes – i.e., a membrane-binding domain. Fifth, the structure of the apo-SCP-2 has been examined by fluorescence, NMR, and X-ray crystallography. Sixth, SCP-2 is capable of binding both sterol and fatty acid/acyl CoA-type ligands with high affinity. The latter represent hitherto unrecognized potential functions of SCP-2 in fatty acid metabolism/oxidation. The structure of the SCP-2 fatty acid-binding site has been shown by use of a nitroxide spin-labeled fatty acid and, as shown for the first time here, using the most prevalent fatty acid type occurring in nature, oleic acid. The SCP-2 oleic acid-binding site extends from the region of the two N-terminal α helices, through the space between α helix A and β strand I and exits into the area of β strand IV (fig. 7). This shows that the N-terminal α-amphipathic helix comprises not only a membrane interaction domain, as proposed more than a decade ago [97] and recently demonstrated [70, 71], but also forms an important part of a domain whereby this protein binds fatty acids.

There are many unresolved issues that need to be addressed in future studies. At the gene level, the promoter regions of the SCP-x/pro-SCP-2 are poorly understood and relatively little is known regarding what determines the relative proportion of 58-kDA SCP-x and 15-kDa pro-SCP-2 mRNA transcripts and protein translation products. Although NMR, X-ray crystallography, fluorescence, and circular dichroism have provided in-depth analyses of the structure of the fatty acid-binding site in the 13-kDa SCP-2, similar work needs to be done to resolve the identity of the fatty acyl CoA-, phospholipid-, and cholesterol-binding site(s) in the 13-kDa SCP-2. An important question will be to resolve why the NMR studies detect two ligand-binding sites (differing cholesterol specificity, but not fatty acid or fatty acyl CoA specificity) while the fluorescence studies detect only a single ligand-binding site. With only two publications to date on the structure and ligand-binding site characterization of the 15-kDa pro-SCP-2, much in-depth work needs to be done regarding the ligand specificity and tertiary structure of these site(s) in the 15-kDa pro-SCP-2, whether ligand-binding site occupancy determines the rate of posttranslational proteolytic processing to the mature 13-kDa SCP-2, and on the intracellular localization of this proteolytic processing. Nothing is known regarding the secondary or tertiary structure of the 58-kDa SCP-x. Likewise, we do not yet know whether ligand-induced alterations in 58-kDa SCP-x, 15-kDa pro-SCP-2, and 13-kDa SCP-2 conformation affect the intracellular targeting of these proteins and bound ligands.

Acknowledgement. This work was supported in part by a grant from the USPHS National Institutes of Health (DK 41402).

1 Vahouny G. V., Chanderbhan R., Kharoubi A., Noland B. J., Pastuszyn A. et al. (1987) Sterol carrier and lipid transfer proteins. Adv. Lipid Res. **22:** 83–113
2 Schroeder F., Frolov A., Schoer J., Gallegos A., Atshaves B. P., Stolowich N. J. et al. (1998) Intracellular cholesterol binding proteins, cholesterol transport and membrane domains. In: Intracellular Cholesterol Trafficking, pp. 213–234, Chang T. Y. and Freeman D. A. (eds), Kluwer, Boston
3 Pfeifer S. M., Furth E. E., Ohba T., Chang Y. J., Rennert H., Sakuragi N. et al. (1993) Sterol carrier protein 2: a role in steroid hormone synthesis? J. Steroid Biochem. Mol. Biol. **47:** 167–172
4 Moncecchi D. M., Nemecz G., Schroeder F. and Scallen T. J. (1991) The participation of sterol carrier protein-2 (SCP-2) in cholesterol metabolism. In: Physiology and Biochemistry of Sterols, pp. 1–27, Patterson G. W. and Nes W. D. (eds), American Oil Chemists' Society Press, Champaign
5 Pfeifer S. M., Sakuragi N., Ryan A., Johnson A. L., Deeley R. G., Billheimer J. T. et al. (1993) Chicken sterol carrier protein 2/sterol carrier protein x: cDNA cloning reveals evolutionary conservation of structure and regulated expression. Arch. Biochem. Biophys. **304:** 287–293
6 Tan H., Okazaki K., Kubota I., Kamiryo T. and Utiyama H. (1990) A novel peroxisomal nonspecific lipid-transfer protein from *Candida tropicalis*: gene structure, purification and possible role in beta-oxidation. Eur. J. Biochem. **190:** 107–112
7 Meijer E. A., DeVries S. C., Steck P., Gadella D. W. J., Wertz K. W. A. and Hendricks T. (1993) Characterization of the nonspecific lipid transfer protein EP2 from carrot (*Daucus carota* L.). Mol. Cell. Biochem. **123:** 159–166
8 Subirade M., Salesse C., Marion D. and Pezolet M. (1995) Interaction of nonspecific wheat lipid transfer protein with phospholipid monolayers imaged by fluorescence microscopy and studied by infrared spectroscopy. Biophys. J. **69:** 974–988
9 Desormeaux A., Blochet J. E., Pezolet M. and Marion D. (1992) Amino acid sequence of a non-specific wheat phospholipid transfer protein and its conformation as revealed by infrared and Raman spectroscopy: role of disulfide bridges and phospholipids in the stabilization of the α-helix structure. Biochim. Biophys. Acta **1121:** 137–152
10 Gincel E., Simorre J. P., Caille A., Marion D., Ptak M. and Vovelle F. (1994) Three-dimensional structure in solution of a wheat lipid-transfer protein from multidimensional ^{1}H-NMR data. Eur. J. Biochem. **226:** 413–422
11 Schroeder F., Butko P., Nemecz G. and Scallen T. J. (1990) Interaction of fluorescent delta 5,7,9(11),22-ergostatetraen-3β-ol with sterol carrier protein-2. J. Biol. Chem. **265:** 151–157
12 Colles S. M., Woodford J. K., Moncecchi D., Myers-Payne S. C., McLean L. R., Billheimer J. T. et al. (1995) Cholesterol interactions with recombinant human sterol carrier protein-2. Lipids **30:** 795–804
13 Sams G. H., Hargis B. M. and Hargis P. S. (1991) Identification of two lipid binding proteins from liver of *Gallus domesticus*. Comp. Biochem. Physiol. **99B:** 213–219
14 Stolowich N. J., Frolov A., Petrescu A. D., Scott A. I., Billheimer J. T. and Schroeder F. (1999) Holo-sterol carrier protein-2: ^{13}C-NMR investigation of cholesterol and fatty acid binding sites. J. Biol. Chem. **274:** 35425–35433
15 Seedorf U., Raabe M., Ellinghaus P., Kannenberg F., Fobker M., Engel T. et al. (1998) Defective peroxisomal catabolism of branched fatty acyl coenzyme A in mice lacking the sterol car-

rier protein-2/sterol carrier protein-x gene function. Genes Dev. **12:** 1189–1201
16 Moncecchi D. M., Murphy E. J., Prows D. R. and Schroeder F. (1996) Sterol carrier protein-2 expression in mouse L-cell fibroblasts alters cholesterol uptake. Biochim. Biophys. Acta **1302:** 110–116
17 Atshaves B. P., Petrescu A., Starodub O., Roths J., Kier A. B. and Schroeder F. (1999) Expression and intracellular processing of the 58 kDa sterol carrier protein 2/3-oxoacyl-CoA thiolase in transfected mouse L-cell fibroblasts. J. Lipid Res. **40:** 610–622
18 Hirai A., Kino T., Tokinaga K., Tahara K., Tamura Y. and Yoshida S. (1994) Regulation of sterol carrier protein 2 (SCP2) gene expression in rat peritoneal macrophages during foam cell formation. J. Clin. Invest. **94:** 2215–2223
19 Lipka G., Schulthess G., Thurnhofer H., Wacker H., Wehrli E., Zeman K. et al. (1995) Characterization of lipid exhange proteins isolated from small intestinal brush border membrane. J. Biol. Chem. **270:** 5917–5925
20 Schulthess G., Lipka G., Compassi S., Boffelli D., Weber F. E., Paltauf F. et al. (1994) Absorption of monoacylglycerols by small intestinal brush border membrane. Biochemistry **33:** 4500–4508
21 Puglielli L., Rigotti A., Greco A. V., Santos M. J. and Nervi F. (1995) Sterol carrier protein-2 is involved in cholesterol transfer from the endoplasmic reticulum to the plasma membrane in human fibroblasts. J. Biol. Chem. **270:** 18723–18726
22 Murphy E. J. and Schroeder F. (1997) Sterol carrier protein-2 mediated cholesterol esterification in transfected L-cell fibroblasts. Biochim. Biophys. Acta **1345:** 283–292
23 Chao H., Billheimer J. T., Kier A. B. and Schroeder F. (1999) Microsomal long chain fatty acyl CoA transacylation: differential effect of SCP-2. Biochim. Biophys. Acta **1439:** 371–383
24 Yamamoto R., Kallen C. B., Babalola G. O., Rennert H., Billheimer J. T. and Strauss J. F. I. (1991) Cloning and expression of a cDNA encoding human sterol carrier protein 2. Proc. Natl. Acad. Sci. USA **88:** 463–467
25 Chanderbhan R., Kharroubi A., Noland B. J., Scallen T. J. and Vahouny G. V. (1986) Sterol carrier protein 2: further evidence for its role in adrenol steroidogenesis. Endocr. Res. **12:** 351–370
26 Chanderbhan R. F., Kharroubi A., Pastuszyn A., Gallo L. L. and Scallen T. (1998) Direct evidence for sterol carrier protein-2 (SCP-2) participation in ACTH stimulated steroidogenesis in isolated adrenal cells. In: Intracellular Cholesterol Trafficking, pp. 197–212, Chang T. Y. and Freeman D. A. (eds), Kluwer, Boston
27 Batenburg J. J., Ossendorp B. C., Snoek G. T., Wirtz K. W., Houweling M. and Elfring R. H. (1994) Phospholipid-transfer proteins and their mRNAs in developing rat lung and in alveolar type-II cells. Biochem. J. **298:** 223–229
28 Puglielli L., Rigotti A., Amigo L., Nunez L., Greco A. V., Santos M. J. et al. (1996) Modulation of intrahepatic cholesterol trafficking: evidence by in vivo antisense treatment for the involvement of sterol carrier protein-2 in newly synthesized cholesterol transfer into bile. Biochem. J. **317:** 681–687
29 Fuchs M., Lammert F., Wang D. Q. H., Paigen B., Carey M. C. and Cohen D. E. (1998) Sterol carrier protein-2 participates in hypersecretion of biliary cholesterol during cholesterol gallstone formation in genetically gallstone susceptible mice. Biochem. J. **336:** 33–37
30 Ito T., Kawata S., Imai Y., Kakimoto H., Trzaskos J. and Matsuzawa Y. (1996) Hepatic cholesterol metabolism in patients with cholesterol gallstones: enhanced intracellular transport of cholesterol. Gastroenterology **110:** 1619–1627
31 Frolov A., Cho T. H., Billheimer J. T. and Schroeder F. (1996) Sterol carrier protein-2, a new fatty acyl coenzyme A-binding protein. J. Biol. Chem. **271:** 31878–31884
32 Schroeder F., Myers-Payne S. C., Billheimer J. T. and Wood W. G. (1995) Probing the ligand binding sites of fatty acid and sterol carrier proteins: effects of ethanol. Biochemistry **34:** 11919–11927
33 Stolowich N. J., Frolov A., Atshaves B. P., Murphy E., Jolly C. A., Billheimer J. T. et al. (1997) The sterol carrier protein-2 fatty acid binding site: an NMR, circular dichroic, and fluorescence spectroscopic determination. Biochemistry **36:** 1719–1729
34 Frolov A., Miller K., Billheimer J. T., Cho T.-C. and Schroeder F. (1997) Lipid specificity and location of the sterol carrier protein-2 fatty acid binding site: a fluorescence displacement and energy transfer study. Lipids **32:** 1201–1209
35 Starodub O., Jolly C. A., Atshaves B. P., Roths J. B., Murphy E. J., Kier A. B. et al. (2000) Sterol carrier protein-2 immunolocalization in endoplasmic reticulum and stimulation of phospholipid formation. Am. J. Physiol. **279:** C1259–C1269
36 Zanlungo S., Amigo L., Mendoza H., Glick J., Rodriguez A., Kozarsky K. et al. (2000) Overexpression of sterol carrier protein-2 in mice leads to increased hepatic cholesterol content and enterohepatic circulation of bile acids. Gastroenterology **118:** 135
37 Seedorf U. (1998) Functional analysis of sterol carrier protein-2 (SCP2) in SCP2 knockout mouse. In: Intracellular Cholesterol Trafficking, pp. 233–252, Chang T. Y. and Freeman D. A. (eds), Kluwer, Boston
38 Ossendorp B. C., Voorhout W. F., Amerongen A. van, Brunink F., Batenburg J. J. and Wirtz K. W. A. (1996) Tissue-specific distribution of a peroxisomal 46-kDa protein related to the 58-kDa protein (sterol carrier protein X; sterol carrier protein 2/3-oxoacyl-CoA thiolase). Arch. Biochem. Biophys. **334:** 251–260
39 McLean M. P., Billheimer J. T., Warden K. J. and Irby R. B. (1995) Differential expression of hepatic sterol carrier proteins in the streptozotocin-treated diabetic rat. Endocrinology **136:** 3360–3368
40 McLean M. P., Warden K. J., Sandoff T. W., Irby R. B. and Hales D. B. (1996) Altered ovarian sterol carrier protein-2 expression in pregnant streptozotocin treated diabetic rat. Biol. Reprod. **55:** 38–46
41 McLean M. P., Zhao Z. and Ness G. C. (1995) Reduced hepatic LDL-receptor, 3-hydroxy-3-methylglutaryl CoA reductase and sterol carrier protein-2 is associated with pregnancy loss in the diabetic rat. Biol. Reprod. **3:** 695–703
42 Wirtz K. W. A. (1997) Phospholipid transfer proteins revisited. Biochem. J. **324:** 353–360
43 Heusden G. P. H. van, Bos K., Raetz C. R. and Wirtz K. W. A. (1990) Chinese hamster ovary cells deficient in peroxisomes lack the nonspecific lipid transfer protein (sterol carrier protein 2). J. Biol. Chem. **265:** 4105–4110
44 Roff C. F., Pastuszyn A., Strauss J. F. I., Billheimer J. T., Vanier M. T., Brady R. O. et al. (1992) Deficiencies in sex-regulated expression and levels of two hepatic sterol carrier proteins in a murine model of Niemann-Pick type C disease. J. Biol. Chem. **267:** 15902–15908
45 Kawata S., Imai Y., Inada M., Inui M., Kakimoto H., Fukuda K. et al. (1991) Modulation of cholesterol 7-α hydroxylase activity by nsLTP in human liver – possibly altered regulation of cytosolic level in patients with gallstones. Clin. Chim. Acta **197:** 201–208
46 Muench C., Hafer A., Katzberg N., Scheibner J., Stange E. F., Seedorf U. et al. (2000) Relevance of the sterol carrier protein-2 gene for bile acid synthesis and gallstone formation in genetically susceptible mice. Gastroenterology 118, 1166
47 Bun-ya M., Maebuchi M., Kamiryo T., Kurosawa T., Sato M., Tohma M. et al. (1998) Thiolase involved in bile acid formation. J. Biochem **123:** 347–352
48 Ferdinandusse S., Denis S., Berkel E. van, Dacremont G. and Wanders R. J. (2000) Peroxisomal fatty acid oxidation disorders and 58 kDa sterol carrier protein-x (SCP=x): activity

measurements in liver and fibroblasts using a newly developed method. J. Lipid. Res. **41:** 336–342
49 Wanders R. J., Denis S., Berkel E. van, Wouters F., Wirtz K. W. A. and Seedorf U. (1998) Identification of the newly discovered 58 kDa peroxisomal thiolase SCP-x as the main thiolase involved in both pristanic acid and trihydroyxycholestanoid acid oxidation: implications for peroxisomal beta-oxidation disorders. J. Inherit. Metab. Dis. **21:** 302–305
50 Gadella T. W. J., Bastiaens P. I. H., Visser A. J. W. G. and Wirtz K. W. A. (1991) Shape and lipid binding site of the nonspecific lipid transfer protein (sterol carrier protein 2): a steady state and time-resolved fluorescence study. Biochemistry **30:** 5555–5564
51 Schroeder F., Frolov A., Starodub O., Russell W., Atshaves B. P., Petrescu A. D. et al. (2000) Pro-sterol carrier protein-2: role of the N-terminal presequence in structure, function, and peroxisomal targeting. J. Biol. Chem. **275:** 25547–25555
52 Gallegos A. M., Atshaves B. P., Storey S. M., Starodub O., Petrescu A. D., Huang H. et al. (2001) Gene structure, intracellular localization, and functional roles of sterol carrier protein-2. Prog. Lipid Res **40:** 498–563
53 Ohba T., Rennert H., Pfeifer S. M., He Z., Yamamoto R., Holt J. A. et al. (1994) The structure of the human sterol carrier protein X/sterol carrier protein 2 gene (SCP2). Genomics **24:** 370–374
54 Ohba T., Holt J. A., Billheimer J. T. and Strauss J. F. I. (1995) Human sterol carrier protein x/sterol carrier protein 2 gene has two promoters. Biochemistry **34:** 10660–10668
55 Seedorf U. and Assmann G. (1991) Cloning, expression and nucleotide sequence of rat liver sterol carrier protein-2 cDNAs. J. Biol. Chem. **266:** 630–636
56 Ossendorp B. C., Heudsen P. H. V. van and Wirtz K. W. A. (1990) Amino acid sequence of rat liver non-specific lipid transfer protein (sterol carrier protein-2) is present in a high molecular weight protein: evidence from cDNA Analysis. Biochem. Biophys. Res. Commun. **168:** 631–636
57 Moncecchi D. M., Pastuszyn A. and Scallen T. J. (1991) cDNA sequence and bacterial expression of mouse liver sterol carrier protein-2. J. Biol. Chem. **266:** 9885–9892
58 Kesav S., Moncecchi D. M. and Scallen T. J. (1990) Rat liver SCP-cDNA sequence and mRNA expression in rat liver and adrenals. FASEB J. **4:** 732
59 Seedorf U., Raabe U. and Assmann G. (1993) Cloning, expression and sequence of SCP-X encoding cDNAs and a related pseudogene. Gene **123:** 165–172
60 Mori T., Tsukamoto T., Mori H., Tashiro Y. and Fujiki Y. (1991) Molecular cloning and deduced amino acid sequence of nonspecific lipid transfer protein (sterol carrier protein 2) of rat liver: a higher molecular mass (60 kDa) protein contains the primary sequence of nonspecific lipid transfer protein as its C-terminal part. Proc. Natl. Acad. Sci. USA **88:** 4338–4342
61 Billheimer J. T., Strehl L. L., Davis G. L., Strauss III J. F. and Davis L. G. (1990) Characterization of a cDNA encoding rat sterol carrier protein-2. DNA Cell Biol. **9:** 159–165
62 Ossendorp B. C., Heusden G. P. van, De Beer A. L., Bos K., Schouten G. L. and Wirtz K. W. A. (1991) Identification of the cDNA clone which encodes the 58-kDa protein containing the amino acid sequence of rat liver non-specific lipid-transfer protein (sterol-carrier protein 2): homology with rat peroxisomal and mitochondrial 3-oxacyl-CoA thiolases. Eur. J. Biochem. **201:** 233–239
63 Seedorf U., Engel T., Assmann G., Leenders F. and Adamski J. (1995) Intrinsic sterol- and phosphatidylcholine transfer activities of 17 beta-hydroxysteroid dehydrogenase type IV. J. Steroid Biochem. Mol. Biol. **55:** 549–553
64 Baum C. L., Reschly E. J., Gayen A. K., Groh M. E. and Schadick K. (1997) Sterol carrier protein-2 overexpression enhances sterol cycling and inhibits cholesterol ester synthesis and high density lipoprotein cholesterol secretion. J. Biol. Chem. **272:** 6490–6498
65 Szyperski T., Scheek S., Johansson J., Assmann G., Seedorf U. and Wuthrich K. (1993) NMR determination of the secondary structure and the three-dimensional polypeptide backbone fold of the human sterol carrier protein 2. FEBS Lett. **335:** 18–26
66 Garcia F. L., Szyperski T., Dyer J. H., Choinowski T., Seedorf U., Hauser H. et al. (2000) NMR structure of the sterol carrier protein-2: implications for the biological role. J. Mol. Biol. **295:** 595–603
67 Weber F. E., Dyer J. H., Garcia F. L., Werder M., Szyperski T., Wuthrich K. et al. (1998) In pre-sterol carrier protein 2 (SCP2) in solution the leader peptide is flexibly disordered, and residues 21–143 adopt the same globular fold as in mature SCP-2. Cell. Mol. Life Sci. **54:** 751–759
68 Choinowski T., Dyer J. H., Maderegger B., Winterhalter K. M., Hauser H. and Piotnek K. (1999) Crystallization and initial X-ray analysis of rabbit mature sterol carrier protein 2. Acta Crystallogr. **D55:** 1478–1480
69 Choinowski T., Hauser H. and Piotnek K. (2000) Structure of sterol carrier protein 2 at 1.8 Å resolution reveals a hydrophobic tunnel suitable for lipid binding. Biochemistry **39:** 1897–1902
70 Huang H., Ball J. A., Billheimer J. T. and Schroeder F. (1999) The sterol carrier protein-2 amino terminus: a membrane interaction domain. Biochemistry **38:** 13231–13243
71 Huang H., Ball J. A., Billheimer J. T. and Schroeder F. (1999) Interaction of the N-terminus of sterol carrier protein-2 with membranes: role of membrane curvature. Biochem. J. **344:** 593–603
72 Seedorf U., Scheek S., Engel T., Steif C., Hinz H. J. and Assmann G. (1994) Structure-activity studies of human sterol carrier protein 2. J. Biol. Chem. **269:** 2613–2618
73 Jatzke C., Hinz H. J., Seedorf U. and Assmann G. (1999) Stability and binding properties of wild-type and c17s mutated human sterol carrier protein 2. Biochim. Biophys. Acta **1432:** 265–274
74 Hapala I., Kavecansky J., Butko P., Scallen J., Joiner C. and Schroeder F. (1994) Regulation of membrane cholesterol domains by sterol carrier protein-2. Biochemistry **33:** 7682–7690
75 Cistola D. P., Walsh M. T., Corey R. P., Hamilton J. A. and Brecher P. (1988) Interactions of oleic acid with liver fatty acid binding protein: a carbon-13 NMR study [published erratum appears in Biochemistry (1989) **28:** 3628]. Biochemistry **27:** 711–717
76 Matsuura J. E., George H. J., Ramachandran N., Alvarez J. G., Strauss J. F. I. and Billheimer J. T. (1993) Expression of the mature and the pro-form of human sterol carrier protein 2 in *Escherichia coli* alters bacterial lipids. Biochemistry **32:** 567–572
77 Schagger H. and Jagow G. von (1987) Tricine-sodium dodecyl sulfate-polyacrylamide gel electrophoresis for the separation of proteins in the range from 1 to 100 kDa. Anal. Biochem. **166:** 368–379
78 Hubbell T., Behnke W. D., Woodford J. K. and Schroeder F. (1994) Recombinant liver fatty acid binding protein interactions with fatty acyl-coenzyme A. Biochemistry **33:** 3327–3334
79 Jolly C. A., Hubbell T., Behnke W. D. and Schroeder F. (1997) Fatty acid binding protein: stimulation of microsomal phosphatidic acid formation. Arch. Biochem. Biophys. **341:** 112–121
80 McArthur M. J., Atshaves B. P., Frolov A., Foxworth W. D., Kier A. B. and Schroeder F. (1999) Cellular uptake and intracellular trafficking of long chain fatty acids. J. Lipid. Res. **40:** 1371–1383
81 Scallen T. J., Noland B. J., Gavey K. L., Bass N. M., Ockner R. K., Chanderbhan R. et al. (1985) Sterol carrier protein 2 and

fatty acid-binding protein: separate and distinct physiological functions. J. Biol. Chem. **260:** 4733–4739
82 Avdulov N. A., Chochina S. V., Igbavboa U., Warden C. H., Schroeder F. and Wood W. G. (1999) Lipid binding to sterol carrier protein-2 is inhibited by ethanol. Biochim. Biophys. Acta **1437:** 37–45
83 Dansen T. B., Westerman J., Wouters F., Wanders R. J., Hoek A. van, Gadella T. W. et al. (1999) High affinity binding of very long chain fatty acyl CoA esters to the peroxisomal non-specific lipid transfer protein (SCP-2). Biochem. J. **339:** 193–199
84 Glatz J. F. C., Vork M. M., Cistola D. P. and Van der Vusse G. J. (1993) Cytoplasmic fatty acid binding proteins: significance for intracellular transport of fatty acids and putative role on signal transduction pathways. Prost. Leuko. Essen. Fatty Acids **48:** 33–41
85 Gossett R. E., Frolov A. A., Roths J. B., Behnke W. D., Kier A. B. and Schroeder F. (1996) Acyl Co A binding proteins: multiplicity and function. Lipids **31:** 895–918
86 Avdulov N. A., Chochina S. V., Myers-Payne S., Hubbell T., Igbavboa U., Schroeder F. et al. (1998) Expression and lipid binding of sterol carrier protein-2 and liver fatty acid binding proteins: differential effects of ethanol in vivo and in vitro. In: Essential Fatty Acids and Eicosanoids: Invited Papers from the Fourth International Congress, pp. 324–327, Riemersma R. A. K. (ed), American Oil Chemists Society Press, Champaign
87 Nichols J. W. (1987) Binding of fluorescent-labeled phosphatidylcholine to rat liver non-specific lipid transfer protein. J. Biol. Chem. **29:** 14172–14177
88 Gadella T. W. Jr and Wirtz K. W. (1991) The low-affinity lipid binding site of the non-specific lipid transfer protein: implications for its mode of action. Biochim. Biophys. Acta **1070:** 237–245
89 Gadella T. W. and Wirtz K. W. (1994) Phospholipid binding and transfer by non-specific lipid transfer protein (SCP-2): a kinetic model. Eur. J. Biochem. **220:** 1019–1028
90 Berkhout T. A., Visser A. J. W. G. and Wirtz K. W. A. (1984) Static and time resolved fluroescence studies of fluorescent phosphatidylcholine bound to the phosphatidylcholine transfer protein. Biochemistry **23:** 1505–1513
91 Loon D. van, Berkhout T. A. and Wirtz K. W. A. (1985) The lipid binding site of the phosphatidylcholine transfer protein from liver. Chem. Phys. Lipids **38:** 29–39
92 Keller G. A., Scallen T. J., Clarke D., Maher P. A., Krisans S. K. and Singer S. J. (1989) Subcellular localization of sterol carrier protein-2 in rat hepatocytes: its primary localization to peroxisomes. J. Cell Biol. **108:** 1353–1361
93 Antonenkov V. D., Veldhoven P. P. van, Waelkens E. and Mannaerts G. P. (1997) Substrate specificities of 3-oxoacyl-CoA thiolase A and sterol carrier protein 2/3-oxoacyl-CoA thiolase purified from normal rat liver peroxisomes. J. Biol. Chem. **272:** 26023–26031
94 Antonenkov V. D., Veldhoven P. P. van and Mannaerts G. P. (2000) Isolation and subunit composition of native sterol carrier protein-2/3-oxoacyl-coenzyme A thiolase from normal rat liver peroxisomes. Protein Exp. Purif. **18:** 249–256
95 Seedorf U., Brysch P., Engel T., Schrage K. and Assmann G. (1994) Sterol carrier protein X is peroxisomal 3-oxoacyl coenzyme A thiolase with intrinsic sterol carrier and lipid transfer activity. J. Biol. Chem. **269:** 21277–21283
96 Woodford J. K., Colles S. M., Myers-Payne S., Billheimer J. T. and Schroeder F. (1995) Sterol carrier protein-2 stimulates intermembrane sterol transfer by direct membrane interaction. Chem. Phys. Lipids **76:** 73–84
97 Pastuszyn A., Noland B. J., Bazan F., Fletterick R. J. and Scallen T. J. (1987) Primary sequence and structural analysis of sterol protein-2 from rat liver: homology with immunoglobins. J. Biol. Chem. **262:** 13219–13227
98 Johnson W. C. (1999) Analyzing protein circular dichroism spectra for accurate secondary structures. Proteins Struct. Funct. Genet. **35:** 307–312
99 King S. M. and Johnson W. C. (1999) Assigning secondary structure from protein coordinate data. Proteins Struct. Funct. Genet. **35:** 313–320
100 Compton L. A. and Johnson W. C. Jr (1986) Analysis of protein circular dichroism spectra for secondary structure using a simple matrix multiplication. Anal. Biochem. **155:** 155–167


To access this journal online:
http://www.birkhauser.ch